

1 **Estimation of Metabolic Dynamics of Restored Seagrass Meadows in a Southeast Asia Islet:**  
2 **Insights from Ex Situ Benthic Incubation**

3 Mariche B. Natividad<sup>123\*</sup>, Jian-Jhih Chen<sup>45\*</sup>, Hsin-Yu Chou<sup>1</sup>, Lan-Feng Fan<sup>1</sup>, Yi-Le Shen<sup>6</sup>, Wen-Chen  
4 Chou<sup>178</sup>

5 <sup>1</sup>Institute of Marine Environment and Ecology, National Taiwan Ocean University, Taiwan

6 <sup>2</sup>Doctoral Degree Program on Ocean Resources and Environmental Changes, College of Ocean Science  
7 and Resources, National Taiwan Ocean University, Taiwan

8 <sup>3</sup>Ecosystems Research and Development Bureau, Laguna, Philippines

9 <sup>4</sup>Department of Marine Environmental Engineering, National Kaohsiung University of Science and  
10 Technology, Taiwan

11 <sup>5</sup>Department of Oceanography, National Sun Yat-Sen University, Taiwan

12 <sup>6</sup>Penghu Fisheries Biology Research Center, FRI, MOA, Taiwan

13 <sup>7</sup>Center of Excellence for the Oceans, National Taiwan Ocean University, Keelung, Taiwan

14 <sup>8</sup>Institute of Marine Biology, National Dong Hwa University, Pingtung, Taiwan

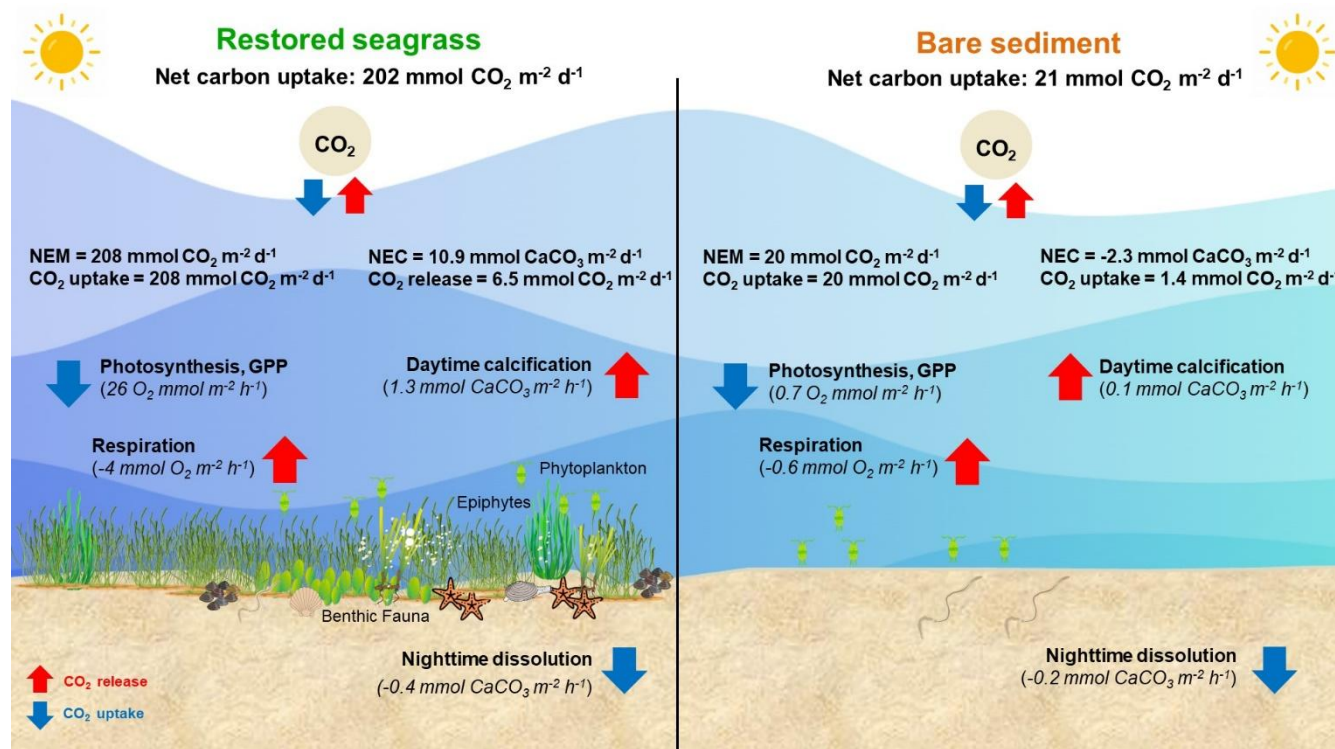
15 *Correspondence to:* Wen-Chen Chou ([wcchou@mail.ntou.edu.tw](mailto:wcchou@mail.ntou.edu.tw))

16 \* These authors contribute equally.

17 **Abstract.** Seagrass meadows are vital carbon sinks, but their function is threatened by rapid decline,  
18 driving restoration efforts to enhance coastal recovery and carbon removal. The capacity of these restored  
19 seagrass as carbon sources or sinks depends largely on organic carbon metabolism and carbonate  
20 dynamics. In this study, we employed ex situ core incubation to investigate the metabolic rates of  
21 replanted seagrasses (SG), including gross primary productivity (GPP), community respiration (R), net  
22 ecosystem metabolism (NEM), and net ecosystem calcification (NEC) in SG and surrounding bare  
23 sediments (BS). SG exhibited higher GPP ( $26.0 \pm 3.4 \text{ mmol O}_2 \text{ m}^{-2} \text{ h}^{-1}$  vs  $0.7 \pm 1.3 \text{ mmol O}_2 \text{ m}^{-2} \text{ h}^{-1}$ ) and  
24 NEM ( $208.2 \pm 22.2 \text{ mmol O}_2 \text{ m}^{-2} \text{ d}^{-1}$  vs  $20.1 \pm 9.9 \text{ mmol O}_2 \text{ m}^{-2} \text{ d}^{-1}$ ) than BS, indicating their potential as  
25 carbon sinks by shifting benthic metabolism toward a more autotrophic state. In contrast, SG exhibited  
26 net calcification with positive NEC values ( $10.9 \pm 15.7 \text{ mmol CaCO}_3 \text{ m}^{-2} \text{ d}^{-1}$ ), driven by higher daytime  
27 carbonate production than nighttime dissolution, while BS showed net dissolution with negative NEC  
28 values ( $-2.3 \pm 18.8 \text{ mmol CaCO}_3 \text{ m}^{-2} \text{ d}^{-1}$ ). Despite this, high variability in carbonate fluxes led to no  
29 significant difference between SG and BS ( $p > 0.05$ ). In summary, our results found that the SG exhibited

30 significantly higher NEM compared to BS ( $p<0.01$ ), while no significant difference was found for NEC.  
 31 Consequently, the net effect on the carbon uptake capacity of the restored seagrass is likely increased,  
 32 primarily due to the higher NEM. Our findings highlight the ecological significance of seagrass  
 33 restoration in mitigating climate change through carbon removal. The ex situ core incubation method  
 34 allows for the simultaneous measurement of organic and inorganic carbon metabolism. While ex situ core  
 35 incubation enhances feasibility, in situ assessments are still necessary to validate the results and ensure a  
 36 comprehensive understanding of seagrass ecosystem dynamics.

37



38

39 **Graphical abstract: Illustration of carbon uptake from organic carbon metabolism (GPP-gross**  
 40 **primary productivity, R-respiration, NEM-net ecosystem metabolism) and carbonate dynamics**  
 41 **(daytime calcification, nighttime dissolution, and NEC-net ecosystem calcification) in restored**  
 42 **seagrass and bare sediment. Net Ecosystem Metabolism (NEM).**

## 43 1 Introduction

44 Seagrass meadows, comprising over 72 species, occupy just 0.1% of the ocean's surface, yet they are  
45 highly productive and ecologically significant ecosystems in the marine environments (Fourqurean et al.,  
46 2012; Short et al., 2011). These meadows play essential roles in nutrient and carbon cycling and serve as  
47 key habitats for many marine species (Duarte et al., 2010; Fourqurean et al., 2012). Due to their relatively  
48 complex structure, seagrass meadows capture and retain organic carbon ( $C_{org}$ ) in the sediment, making  
49 them one of the major carbon reservoirs globally (Duarte et al., 2005; Mcleod et al., 2011). Previous  
50 estimates suggest that seagrasses account for approximately 15% of the total global carbon sequestered  
51 in benthic sediments (Duarte et al., 2013), with burial rates 35 times that of tropical rainforests (Mcleod  
52 et al., 2011).

53

54 In spite of their ecological significance, seagrass meadows have experienced a global decline, driven  
55 primarily by human-induced activities such as coastal development, eutrophication, and deteriorating  
56 water quality (Orth et al., 2006; Waycott et al., 2009). Since 1980, the global coverage of seagrass has  
57 decreased by 110 km<sup>2</sup> annually, with the rate of decline increasing (Waycott et al., 2009). The loss is  
58 frequently associated with increased water column turbidity and epiphytic shading, which reduce the light  
59 for seagrass photosynthesis, leading to meadow degradation (Campbell et al., 2003; Orth et al., 2006).  
60 Degradation also diminishes their capacity to modify local pH and influence the dynamics of dissolved  
61 oxygen (DO) and dissolved inorganic carbon (DIC) (Hendricks et al., 2014). Moreover, the continued  
62 loss of seagrass ecosystems raises concerns that vast amounts of previously sequestered carbon could be  
63 released back in the atmosphere, converting seagrasses from carbon sinks to carbon sources and  
64 intensifying global climate change (Macreadie et al., 2013). The ongoing decline could potentially release  
65 up to 299 Tg of carbon annually, contributing roughly 10% of CO<sub>2</sub> emissions associated with  
66 anthropogenic land-use changes (Fourqurean et al., 2012).

67

68 In response to these challenges, seagrass restoration has emerged as a critical strategy to mitigate  
69 environmental degradation, enhance coastal resilience, and address global climate change (Juska and Berg

et al., 2022). Protecting and restoring seagrass meadows aligns with international goals like the Paris Agreement, as these ecosystems offer significant potential for long-term carbon storage and climate regulation (Fourqurean et al., 2012). However, despite growing restoration efforts, there remains limited understanding of their success, particularly regarding benthic metabolism and carbon dynamics (Kindeberg et al., 2024). While studies from temperate regions, such as the *Zostera marina* restoration in the Virginia Coast (Rheuban et al., 2014), have provided valuable insights, data from tropical regions — including Southeast Asia, a global hotspot for seagrass diversity — remain scarce (Duarte et al., 2010; Ward et al., 2022; Chou et al., 2023). It represents a critical gap in our knowledge of the impact of restoration efforts on carbon removal and ocean acidification mitigation.

Although there is increasing consensus on the potential of “Blue Carbon” storage in seagrass meadows as a climate change mitigation strategy, the biogeochemical cycling within these ecosystems is complex. Several processes, including ecosystem calcification, anaerobic metabolism, and bioturbation, can counteract net organic carbon (OC) sequestration (Van Dam et al., 2021). These processes regulate local DIC and total alkalinity (TA) budgets, adding complexity to accurately quantifying carbon sequestration (Kindeberg et al., 2024). Overlooking these processes can result in significant overestimates of local carbon sequestration rates and misinterpretations of the role seagrass meadows play in mitigating climate change, potentially leading to inaccurate assessments of their carbon sink capacity (Johansen et al., 2023; Chen et al., 2024; Fan et al., 2024).

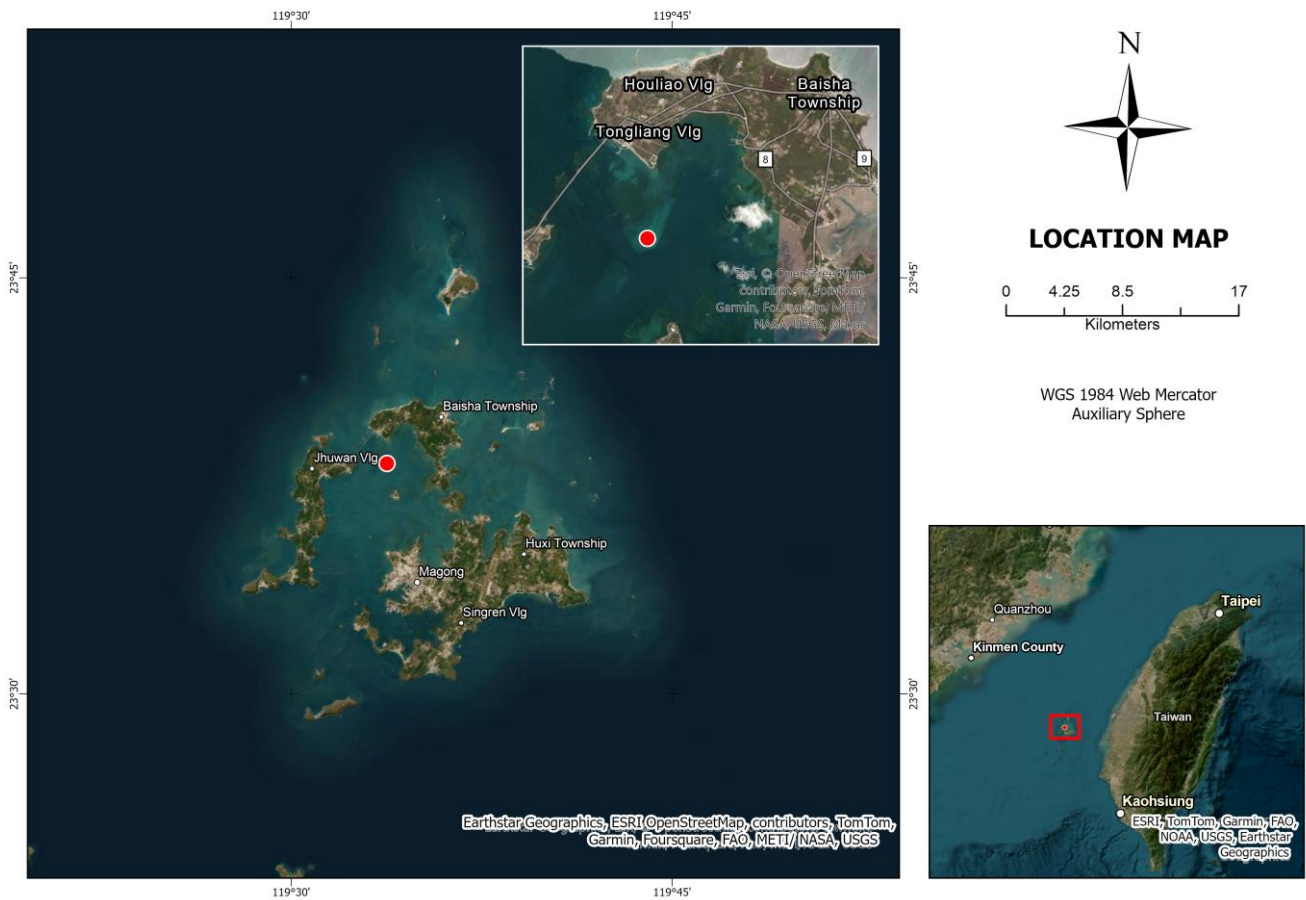
Several methodologies were developed to quantify benthic metabolism, which is a crucial component of biogeochemical cycling, including photosynthesis-irradiance curve (Kraemer and Alberte, 1993), the open water O<sub>2</sub> mass balance approach (Odum, 1956; Chou et al., 2023), and aquatic eddy covariance (Berg et al., 2022; Juska and Berg, 2022). While these methods provide important data, they might overlook the complexities of bioturbation, remineralization, and carbonate dynamics (Olivé et al., 2016; Ward et al., 2022; Juska and Berg, 2022). In this study, we aim to address these knowledge gaps by quantifying organic carbon metabolism (net ecosystem metabolism, NEM) and carbonate dynamics (i.e.,

97 net ecosystem calcification, NEC) in restored seagrass meadows (SG) and adjacent bare sediment (BS)  
98 habitats on a Southeast Asia islet, using an innovative ex situ benthic incubation.

## 99 **2 Materials and Methods**

### 100 **2.1 Study site**

101 The Penghu Islands, located in the southern part of Taiwan Strait (Fig. 1), host a range of seagrass species.  
102 Notably, four species have been reported: *Halophila ovalis*, *Halodule pinifolia*, *Halodule uninervis*, and  
103 *Zostera japonica* (Yang et al., 2002). The sampling location (23° 38' 18.38" N and 119° 33' 46.48" E) is  
104 a restoration meadow dominated by *H. uninervis* and *H. ovalis*. This restoration site encompasses  
105 approximately 3 hectares (Allen Coral Atlas, 2020), with seagrass percent cover varying from 20% to  
106 90%. These seagrasses are subtidal, with water depths ranging from 1.7 meters to 4.4 meters. The  
107 substrate in this area is composed of carbonate sand. The area supports a diverse community of bivalves  
108 (e.g., *Pinna* sp.), gastropods, echinoderms, and various fish species, all of which were observed during  
109 the sampling.



110

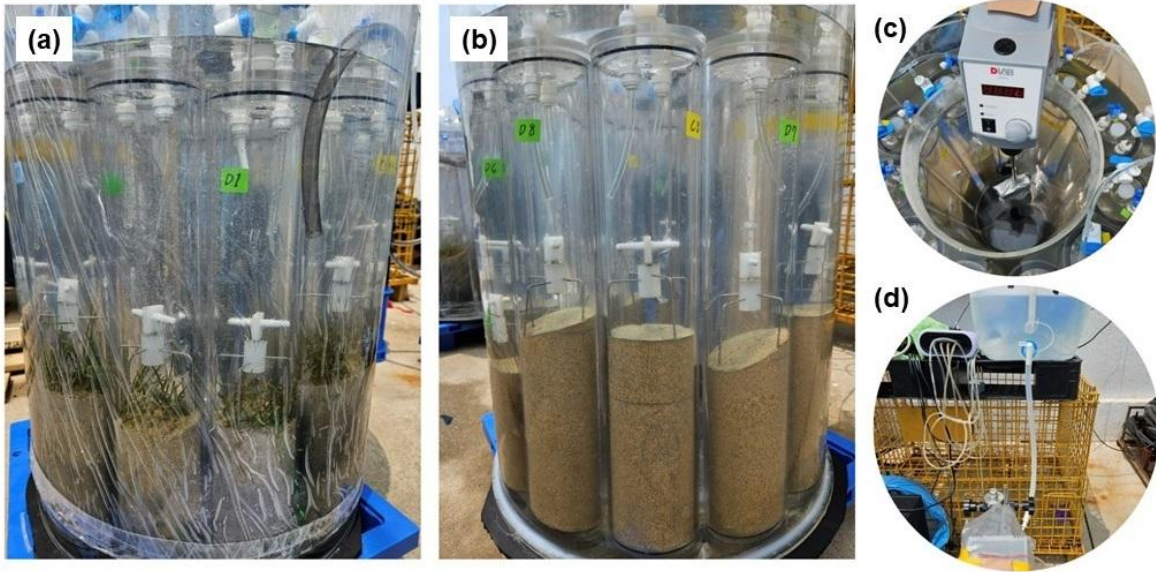
111 **Figure 1: Location map of sampling stations in restored seagrass in Penghu Island, Taiwan (Map**  
 112 **created in ArcGIS Pro. Source: Earthstar Geographics, ESRI OpenStreetMap, Contributors,**  
 113 **TomTom, Garmin, Foursquare, FAO, METI/NASA, USGS, NOAA).**

## 114 2.2 Ex situ core incubation system

115 The ex situ benthic core methodology used in this study was adapted from Chen et al. (2019) (Fig. 2).  
 116 This approach has been widely employed in various studies to assess nutrient concentrations and benthic  
 117 metabolism in coastal ecosystems and estuaries (Eyre & Ferguson, 2005; Maher & Eyre, 2011). Typically,  
 118 the ex situ core incubation involves 150-L treatment tanks containing aerated water. Each tank can  
 119 accommodate 10 plexiglass cores made of polycarbonate material, 10 cm in diameter and 50 cm in height.  
 120 The tanks were equipped with magnetic stir bars driven by a centrally located rotating motor fitted with



121 a magnet. The core has a plexiglass lid which contains two ports, one for probe insertion (Eyre &  
122 Ferguson, 2005). This method offers a feasible approach for quantifying seagrass metabolism, especially  
123 in subtidal systems where in situ measurements are often logistically challenging. While ex situ conditions  
124 may differ from natural underwater environments, we carefully designed our setup to closely replicate  
125 field conditions, including natural light exposure and ambient temperature, to ensure ecological relevance.



126

127 **Figure 2: Ex situ benthic chamber setup for measuring metabolic rates and carbonate dynamics in**  
128 **seagrass meadows and bare sediment. The chambers contain seagrass samples (a), while the**  
129 **chambers contain bare sediment (b). Insets show close-ups of the central rotating motor with a**  
130 **magnet setup for water circulation (c), and the setup for continuous seawater supply (d).**

131 **2.3 Sediment core collection and pre-incubation**

132 The incubation was conducted on April 12-13, 2024. Twenty intact sediment cores, comprising both  
133 seagrass and bare sediment, were collected on-site using the plexiglass tubes. The cores were inserted  
134 about 20 cm into the sediment, keeping approximately 1.9 liters of water. Each core was sealed with a  
135 gas-tight plexiglass plate at the bottom. The samples were brought back to the incubation site within two  
136 hours of collection and allowed to settle for 24 hours. Additionally, 150 liters of water were collected on-  
137 site for continuous supply during the experiment.

138

139 At the incubation site, the cores were uncovered and placed in 150-liter tanks filled with aerated seawater.  
140 They were kept at in situ temperature, exposed to natural sunlight, and continuously recirculated. The  
141 stirring rate was controlled to prevent sediment resuspension (Ferguson et al., 2004). The cores underwent  
142 a 24-hour pre-incubation period to promote stable sediment profiles. The seagrass composition within  
143 the collected cores for ex situ core incubation was dominated by *H. uninervis* and *H. ovalis*. The shoot  
144 count of *H. uninervis* ranged from 20 to 40 shoots per 0.008 m<sup>2</sup>, while *H. ovalis* ranged from 2 to 20  
145 shoots per 0.008 m<sup>2</sup>.

#### 146 **2.4 Sample collection and analysis**

147 Following pre-incubation, the cores were tightly closed using a plexiglass lid. Temperature, salinity, and  
148 pH were determined using a YSI ProDSS Multiparameter water quality sonde, while DO (mg l<sup>-1</sup>) was  
149 measured with a thermo DO probe. Both probes were calibrated with calibration standards. Measurements  
150 were taken at midnight (24:00 h) with 2-hour intervals and ended at noon. Photosynthetically active  
151 radiation (PAR) levels were measured using SQ-420X Smart Quantum Sensor positioned atop the  
152 incubation tank.

153

154 After measurements, three 150 ml seawater samples were collected separately from the SG and BS cores  
155 using a syringe for DIC and pH analysis. The water samples were processed with 60 µL HgCl<sub>2</sub> solution  
156 to stop any biological activity. DIC analysis was performed using a non-dispersive infrared method with  
157 a DIC analyzer (AS-C3, Apollo SciTech Inc.), following the approach of Dickson et al. (2007) and our  
158 past studies (Chou et al., 2018; 2021; Fan et al., 2024). For each DIC run, we used certified reference  
159 material (Batch no. 206) sourced from A. G. Dickson at Scripps Institution of Oceanography to check for  
160 drift and systematic bias. pH values were measured spectrophotometrically in total scale at 25 °C  
161 following Clayton and Byrne (1993). Data from DIC and pH, along with actual temperature and salinity,  
162 were used to calculate the TA, partial pressure of CO<sub>2</sub> (*p*CO<sub>2</sub>), and aragonite saturation state ( $\Omega_{Ar}$ ) using  
163 the Excel macro CO2SYS version 2.1 (Pelletier et al. 2011). The dissociation constants for carbonic acid



164 applied in these calculations were obtained from Mehrbach et al. (1973) and subsequently refined by  
165 Dickson and Millero (1987).

## 166 **2.5 Benthic flux rate calculations**

167 Areal rates of R, GPP, NPP, and NEM were calculated based on changes in DO concentrations, following  
168 equation 1 (Eyre et al. 2011). Respiration rates were determined from concentration data collected during  
169 the initial dark period (midnight to dawn) (eq. 2). NPP was calculated based on light O<sub>2</sub> flux  
170 measurements from dawn to noon (eq. 3). We implemented a 6-hour dark incubation period to ensure  
171 oxygen concentrations remained above 80% (Eyre et al., 2002) and a 6-hour light incubation period to  
172 prevent oxygen from reaching supersaturated levels (Olivé et al., 2016). Hourly GPP rates were computed  
173 as the difference between R and NPP rates (eq. 4). NEM was calculated using equation 5. Positive values  
174 indicate autotrophic, while negative values represent heterotrophic.

$$175 \quad F = [(C_{t1} - C_{t0}) \times V/A]/T \quad (\text{eq. 1})$$

176 Where F = flux rate ( $\mu\text{mol m}^{-2} \text{h}^{-1}$ ), C<sub>t0</sub> and C<sub>t1</sub> = concentration in the overlying water at the start and end  
177 of the time period ( $\mu\text{mol l}^{-1}$ ), respectively, V = volume of overlying water in the core (l), A = surface area  
178 in the sediment core (m<sup>2</sup>), and T = incubation period (h).

$$179 \quad R = \text{dark O}_2 \text{ flux (negative)} \quad (\text{eq. 2})$$

$$180 \quad \text{NPP} = \text{light O}_2 \text{ flux (positive)} \quad (\text{eq. 3})$$

$$181 \quad \text{GPP} = \text{NPP (positive)} - R \text{ (negative)} \quad (\text{eq. 4})$$

$$182 \quad \text{NEM} = (\text{GPP} \times 12) - (R \times 24 \text{ h} \times -1) \quad (\text{eq. 5})$$

183

184 NEC rates ( $\text{mmol CaCO}_3 \text{ m}^{-2} \text{h}^{-1}$ ) were estimated from the change of total alkalinity, assuming these  
185 changes are only due to CaCO<sub>3</sub> precipitation and dissolution (eq. 6) (Roth et al., 2019; Van Dam et al.,  
186 2019):

$$187 \quad \text{NEC} = -0.5 \frac{\Delta n\text{TA}}{\Delta t} \times hp \quad (\text{eq. 6})$$

188 Here,  $\Delta n\text{TA}$  = change in  $n\text{TA}$  ( $n\text{TA} = \text{TA} \times \text{SSS}_{\text{average}}/\text{SSS}$ ) over the  $\Delta t$  (time), h = volume/area, and  $p$  =  
189 water density. The  $-0.5$  scalar factor was applied to account for the stoichiometric relationship, where 2

190 moles of TA produce 1 mole of  $\text{CaCO}_3$ . Day and night incubations (lasting 12 hours) were conducted  
191 simultaneously with organic carbon metabolism to obtain daily NEC fluxes. The dark period (midnight  
192 to dawn) was used to measure nighttime dissolution, while the light period (dawn to noon) was used for  
193 daytime calcification. Alkalinity was measured every 3 hours throughout the incubation period. NEC is  
194 positive with TA consumption, indicating  $\text{CaCO}_3$  precipitation, and negative with TA production,  
195 indicating  $\text{CaCO}_3$  dissolution.

196 In this study, both hourly and daily rates were reported. Hourly rates allow us to examine diel variations  
197 in metabolic processes, while daily rates provide an integrated view of overall carbon dynamics,  
198 facilitating comparison with existing literature.

## 199 **2.5 Statistical analysis**

200 Independent sample T-tests were applied to compare metabolic rates (R, NPP, GPP, NEM, NEC) between  
201 SG and BS using SPSS v. 17. Data were subjected to a normality test before performing the analysis.  
202 Least-squares linear regression was employed to assess the correlation between changes in DO in the SG  
203 and BS. The Mann-Whitney U test was applied for carbonate chemistry analysis due to the non-normal  
204 distribution of data.

## 205 **3 Results**

### 206 **3.1 Water quality and carbonate chemistry**

207 Diurnal patterns of water quality and carbonate parameters for SG and BS during the two-day ex situ core  
208 incubation are illustrated in Figs. 3 and 4, respectively. The temperature in both treatments ranged from  
209 22 to 29 °C, while salinity levels spanned from 35 to 36. These values were similar to in situ measurements  
210 obtained from the seagrass beds using a CTD profiler. During the daytime (6:00 AM to 12:30 PM), PAR  
211 levels ranged from  $26 \mu\text{mol m}^{-2} \text{s}^{-1}$  to a peak of  $1662 \mu\text{mol m}^{-2} \text{s}^{-1}$ , with the highest intensities observed  
212 at midday. The average PAR measured  $953 \mu\text{mol m}^{-2} \text{s}^{-1}$  on the first day of incubation, increasing slightly  
213 to  $1026 \mu\text{mol m}^{-2} \text{s}^{-1}$  on the second day. DO saturation levels were more variable in SG than BS, with

214 values ranging from 54% to 224% and 92% to 123%, respectively. DO saturation levels in both treatments  
215 followed a diel pattern, with lower nighttime and higher daytime values.

216

217 Both  $nDIC$  ( $nDIC = DIC \times SSS_{\text{average}}/SSS$ ) and  $pH_T$  displayed greater diurnal fluctuations at SG compared  
218 to the BS. At SG,  $nDIC$  ranged from 1660 to 2118  $\mu\text{mol kg}^{-1}$  (mean  $\pm$  SD:  $1963 \pm 153 \mu\text{mol kg}^{-1}$ ), and  
219 followed a diel pattern.  $pH_T$  ranged from 7.81 to 8.37 at SG (mean  $\pm$  SD:  $7.99 \pm 0.2$ ), following the  
220 opposite trend to  $nDIC$ , with values decreasing at night and increasing during the day. At the BS site,  
221 these parameters were less variable, with  $nDIC$  values ranging from 1948 to 2029  $\mu\text{mol kg}^{-1}$  and  $pH_T$   
222 from 7.84 to 7.99, with mean values of  $1993 \pm 27 \mu\text{mol kg}^{-1}$  and  $7.93 \pm 0.1$ , respectively. Similarly, the  
223 calculated  $nTA$  was also more fluctuating in SG than BS, with mean values of  $2243 \pm 24 \mu\text{mol kg}^{-1}$  and  
224  $2230 \pm 24 \mu\text{mol kg}^{-1}$ , respectively. The calculated  $pCO_2$  displayed a broader range at SG (142 to 762  
225  $\mu\text{atm}$ ; mean  $\pm$  SD:  $510 \pm 231$ ) compared to BS (450 to 699  $\mu\text{atm}$ ; mean  $\pm$  SD:  $524 \pm 82$ ), suggesting a  
226 more dynamic carbon cycling potentially driven by seagrass metabolic activity. The mean  $\Omega_{Ar}$  was higher  
227 in SG ( $3.14 \pm 1$ ) compared to BS ( $2.72 \pm 0.4$ ), indicating more favorable conditions for calcification at  
228 the seagrass site. Mann–Whitney test on carbonate chemistry revealed no significant distinction between  
229 SG and BS ( $pH_T$   $p = 0.713$ ;  $nDIC$   $p = 0.419$ ;  $nTA$   $p = 0.679$ ;  $\Omega_{Ar}$   $p = 0.511$ ).

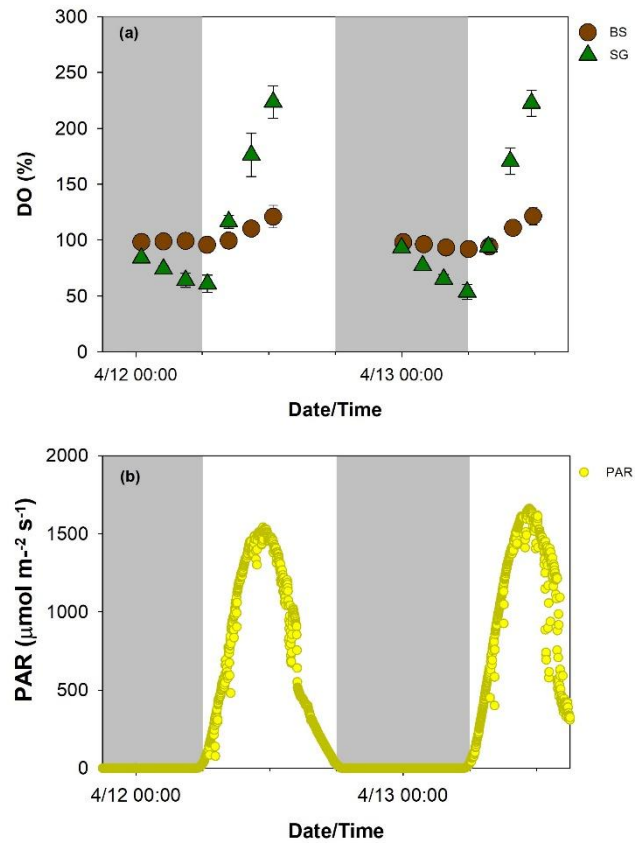


**Figure 3: Diurnal pattern of dissolved oxygen (DO, a) in replanted seagrass (SG, green triangle) and bare sediment (BS, brown circle) (n=9, mean  $\pm$  SD), and photosynthetically active radiation (PAR, b) during the two-day (April 12-13, 2024) incubation.**

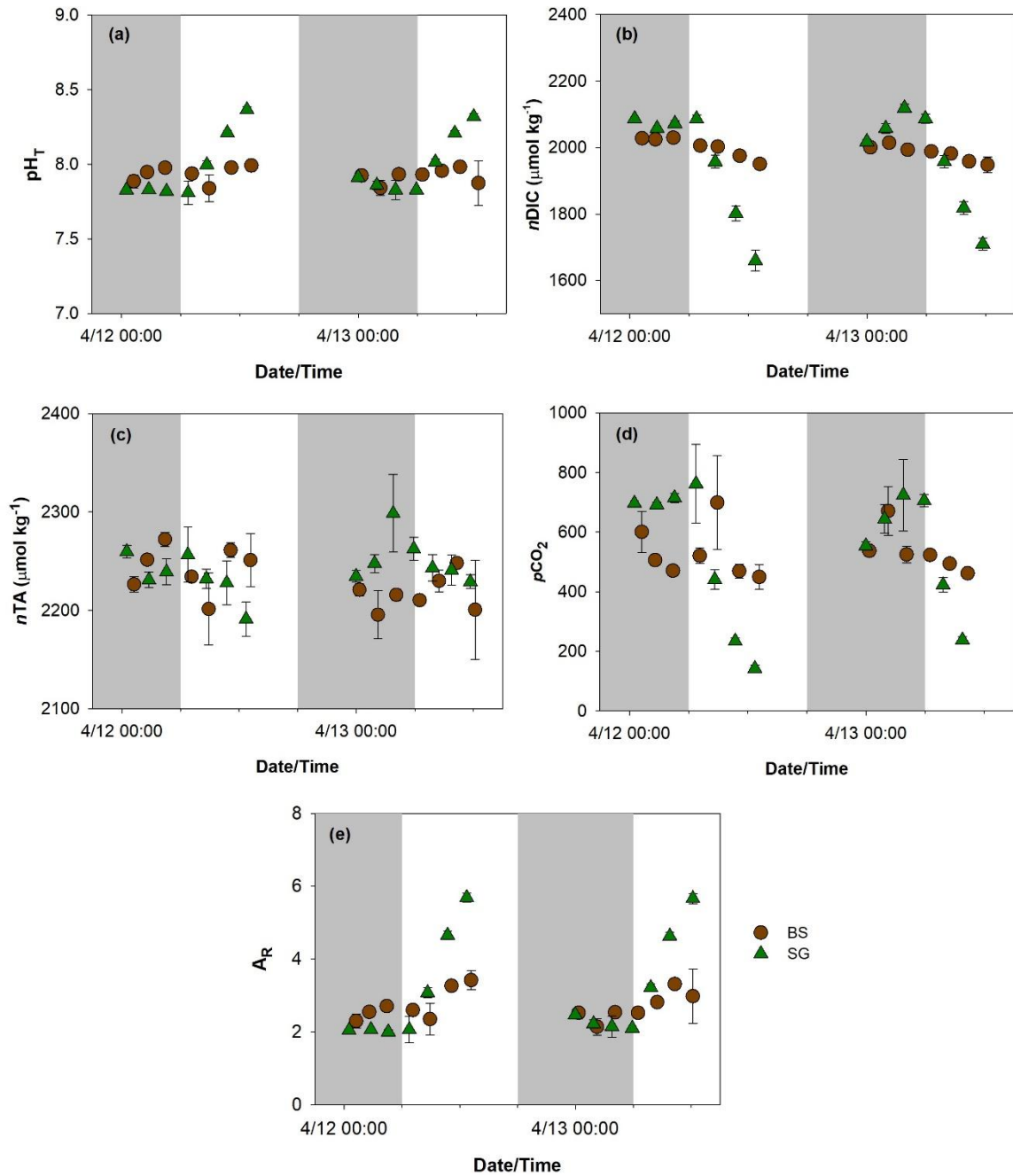


**Figure 4: Total scale pH ( $pH_T$ , a), normalized dissolved inorganic carbon ( $nDIC$ , b), normalized total alkalinity ( $nTA$ , c), partial pressure of carbon dioxide ( $pCO_2$ , d), and aragonite saturation state ( $\Omega_{AR}$ , e) in replanted seagrass (SG, green triangle) and bare sediment (BS, brown circle) during the two-day (April 12-13, 2024) incubation.  $n=3$ , mean  $\pm$  SD.**

### 239 3.2 Respiration, gross primary production, and net ecosystem metabolism

240 Figure 5 illustrates the comparison of metabolic rates (mean  $\pm$  SD) between SG and BS. The mean  
241 respiration rates in SG ( $-4.3 \pm 1.5$  mmol O<sub>2</sub> m<sup>-2</sup> h<sup>-1</sup>) were significantly higher than in BS ( $-0.6 \pm 0.4$  mmol  
242 O<sub>2</sub> m<sup>-2</sup> h<sup>-1</sup>), by approximately 8-fold difference ( $p < 0.01$ ). The mean GPP in SG was  $26.0 \pm 3.4$  mmol O<sub>2</sub>  
243 m<sup>-2</sup> h<sup>-1</sup>, which is 35-fold higher than in BS ( $0.7 \pm 1.3$  mmol O<sub>2</sub> m<sup>-2</sup> h<sup>-1</sup>) ( $p < 0.01$ ). GPP was always higher  
244 than R in both systems, with mean GPP/R ratios of 3.4 and 1.9 in SG and BS, respectively. For NEM,  
245 both systems displayed positive values, indicating net autotrophy, with SG being 10-fold higher ( $208.2 \pm$   
246  $22.2$  mmol O<sub>2</sub> m<sup>-2</sup> d<sup>-1</sup>) compared to BS ( $20.1 \pm 9.9$  mmol O<sub>2</sub> m<sup>-2</sup> d<sup>-1</sup>) ( $p < 0.01$ ). Both R and GPP in SG  
247 and BS increased on the second day of incubation [SG (R:  $-3.1$  vs  $-5.6$  mmol O<sub>2</sub> m<sup>-2</sup> h<sup>-1</sup>; GPP:  $23.3$  vs  
248  $24.7$  mmol O<sub>2</sub> m<sup>-2</sup> h<sup>-1</sup>); BS (R:  $-0.4$  vs  $-0.81$  mmol O<sub>2</sub> m<sup>-2</sup> h<sup>-1</sup>; GPP:  $2.7$  vs  $3.1$  mmol O<sub>2</sub> m<sup>-2</sup> h<sup>-1</sup>)], while  
249 NEM in SG ( $218.04$  vs  $198.4$  mmol O<sub>2</sub> m<sup>-2</sup> d<sup>-1</sup>) and BS ( $22.3$  vs  $17.8$  mmol O<sub>2</sub> m<sup>-2</sup> d<sup>-1</sup>) showed a slight  
250 decrease. However, these changes were not statistically significant.

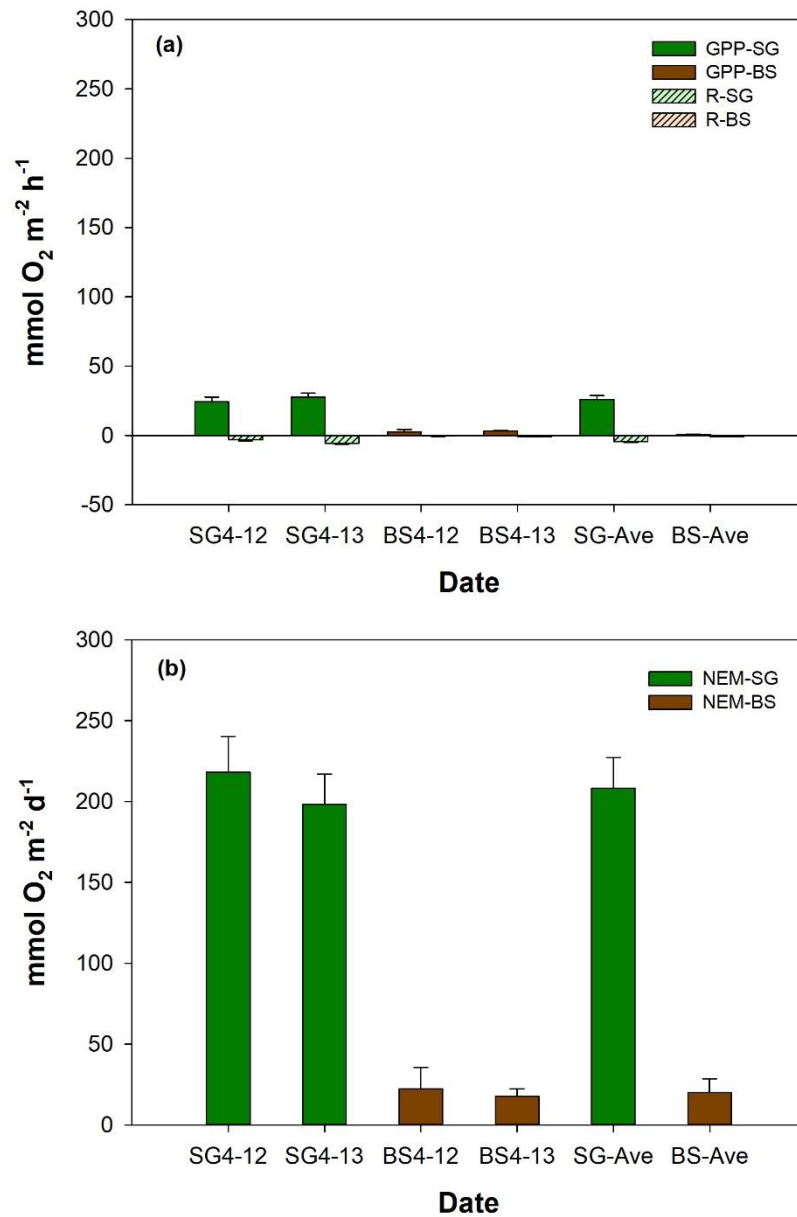


**Figure 5: Mean ( $\pm$  SD, standard deviation) values of (a) metabolic rates such as respiration (R), gross primary productivity (GPP), and (b) net ecosystem metabolism (NEM,) of restored seagrass (SG, green bars) and bare sediment (BS, brown bars) in Penghu during the two-day (April 12-13, 2024) incubation (n=9).**



### 257 **3.2 Calcium carbonate precipitation, dissolution, and net ecosystem calcification**

258 The NEC values (mean  $\pm$  SD) over a diel cycle for SG and BS demonstrated differences in their overall  
259 carbonate dynamics (Fig. 6). Over the two-day incubation period, SG exhibited a net calcifying system  
260 with a mean positive daily NEC means ( $10.9 \pm 15.7$  mmol  $\text{CaCO}_3 \text{ m}^{-2} \text{ d}^{-1}$ ), driven by daytime calcification  
261 ( $1.3 \pm 1.3$  mmol  $\text{CaCO}_3 \text{ m}^{-2} \text{ h}^{-1}$ ) despite nighttime dissolution ( $-0.4 \pm 0.9$  mmol  $\text{CaCO}_3 \text{ m}^{-2} \text{ h}^{-1}$ ). In contrast,  
262 BS supported a net-dissolving system with mean daily NEC ( $-2.3 \pm 18.8$  mmol  $\text{CaCO}_3 \text{ m}^{-2} \text{ d}^{-1}$ ). Mean  
263 daytime calcification and nighttime dissolution were  $0.1 \pm 1.6$  mmol  $\text{CaCO}_3 \text{ m}^{-2} \text{ h}^{-1}$  and  $-0.2 \pm 0.6$  mmol  
264  $\text{CaCO}_3 \text{ m}^{-2} \text{ h}^{-1}$ , respectively. Both systems followed a general diurnal pattern, with positive NEC during  
265 the day (calcifying) and negative at night (dissolving).

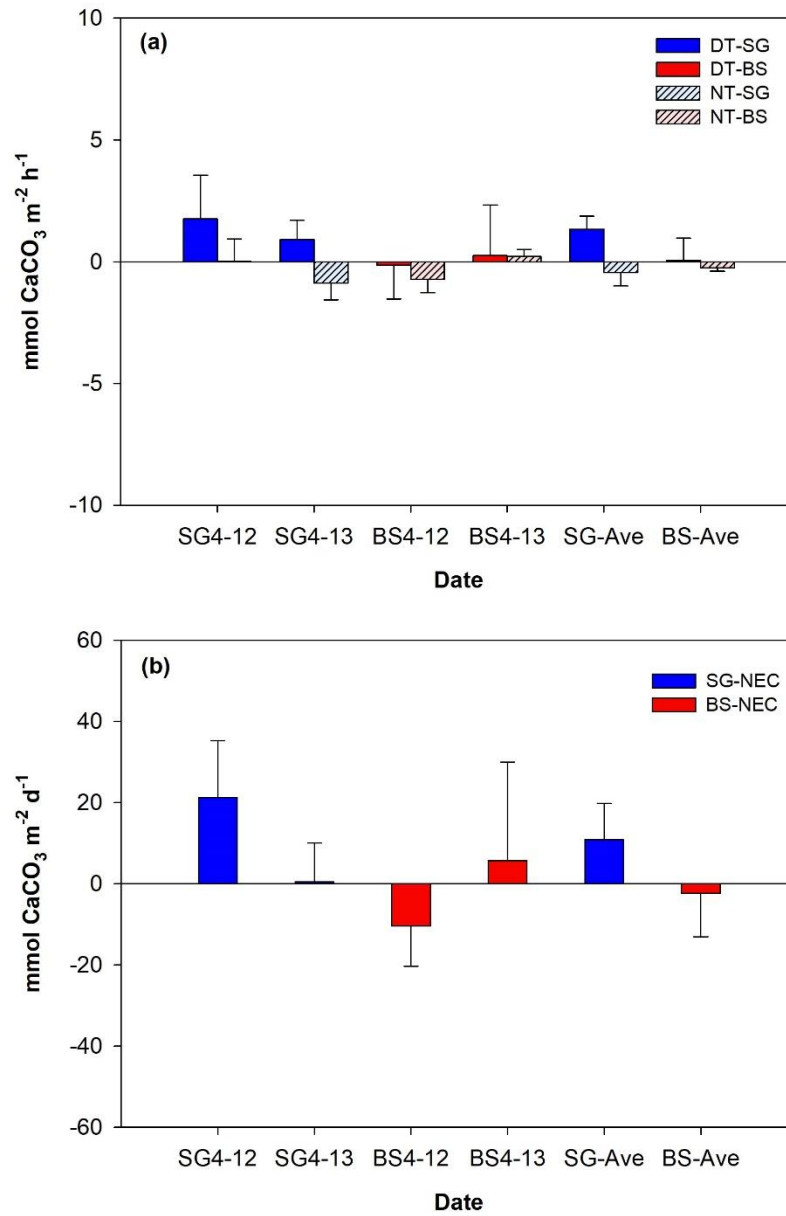


**Figure 6: Mean ( $\pm$  SD, standard deviation) values of daytime (DT) and nighttime (NT) calcification (a), and net ecosystems calcification (NEC, b) of restored seagrass (SG, blue bars) and bare sediment (BS, red bars) in Penghu during the two-day (April 12-13, 2024) incubation (n=3).**

## 270 **4 Discussion**

271 Seagrass meadows are widely recognized as an important blue carbon ecosystem with substantial  
272 potential to mitigate anthropogenic CO<sub>2</sub> emissions. Although research on seagrass ecosystems has grown  
273 in recent years, significant gaps remain in understanding their carbon dynamics. In particular, the balance  
274 of organic and inorganic carbon processes within these systems is not fully understood. Meanwhile, global  
275 seagrass coverage continues to decline, which has increased the urgency of restoration efforts (Waycott  
276 et al. 2009). Restoring seagrass meadows to enhance carbon sequestration has become increasingly  
277 important. Currently, most studies on restored seagrass meadows focus primarily on the burial of  
278 particulate organic carbon (Greiner et al. 2013), with far fewer exploring both organic metabolism and  
279 carbonate cycling in restored seagrass meadows. Here, we present the first dataset on carbon uptake  
280 through metabolic rates and calcification measurements in restored seagrass meadows within tropical  
281 regions.

### 282 **4.1 Restoration of seagrass enhances metabolic rates**

283 The metabolic rates estimated in present study were comparable to those recorded in other seagrass  
284 meadows (Table 1). Our GPP in SG was 24% and 37% higher than the tropical and global averages,  
285 respectively, but 38% lower than Dongsha Island, Taiwan (Chou et al., 2023). It is also comparable to  
286 measurements reported for *H. uninervis* in Tropical Australia (Table 1). Conversely, the R values  
287 estimated in this study were roughly half lower than the tropical and global averages (Duarte et al., 2010).  
288 Our NEM (214 mmol O<sub>2</sub> m<sup>-2</sup> d<sup>-1</sup>) is within the range of previous estimates for tropical seagrass meadows  
289 (-477.28 to 484.20 mmol O<sub>2</sub> m<sup>-2</sup> d<sup>-1</sup>) and global estimates (-477.28 to 531.63 mmol O<sub>2</sub> m<sup>-2</sup> d<sup>-1</sup>). In addition  
290 to these global comparisons, our study reveals a clear distinction in metabolic rates (e.g. GPP, R, NEM)  
291 between SG and BS. The GPP and R in restored seagrass meadows were 35 and 7 times greater than in  
292 BS. The relatively higher metabolic rates in seagrass meadows compared to bare sediments have also  
293 been observed in other studies (Table 1). For instance, a two-year-old restored *Halodule wrightii* meadow  
294 demonstrated a 13-fold increase in NEM relative to bare sediment (Egea et al., 2023). Similarly,  
295 *Posidonia oceanica* exhibited a notable 70-fold increase in metabolic rates compared to bare sediment  
296 (Barron et al., 2006). Furthermore, *Zostera marina* exhibits net autotrophy while bare sediments are net

297 heterotrophy (Attard et al., 2019; Chen et al., 2019). Such patterns highlight the fundamental ecological  
 298 functions restored seagrass meadows play relative to unvegetated/bare sediments. The increase in GPP  
 299 reflects the enhanced carbon fixation capacity of seagrass meadows, while the elevated R indicates active  
 300 organic matter decomposition and microbial respiration (Duarte and Krause-Jensen, 2017). According to  
 301 Duarte et al. (2010), seagrass meadows generally act as autotrophic ( $NEM > 0$ )  $CO_2$  sinks when GPP  
 302 exceeds  $186 \text{ mmol } O_2 \text{ m}^{-2} \text{ d}^{-1}$ , and shift to heterotrophy ( $NEM < 0$ ) when GPP falls below this threshold.  
 303 Based on this threshold, our mean GPP for restored seagrass exceeded the value for autotrophy, resulting  
 304 in a positive NEM which is consistent with their global assessment. The NEM observed in SG was 10  
 305 times higher than in BS, suggesting that SG sequesters significantly more carbon than BS. These findings  
 306 highlight that seagrass restoration significantly boosts metabolic rates and enhances carbon cycling.  
 307 Given the increasing loss of global seagrass cover, restoration not only boosts ecosystem productivity but  
 308 also strengthens the ability of coastal systems to remove carbon, thereby contributing to climate change  
 309 mitigation efforts.  
 310

311 **Table 1. Comparison of metabolic rates from global estimates. GPP and R values are expressed in**  
 312  **$\text{mmol } O_2 \text{ m}^{-2} \text{ h}^{-1}$  units, while NEM in  $\text{mmol } O_2 \text{ m}^{-2} \text{ d}^{-1}$ .**

Location	Method	Seagrass Community	GPP	R	NEM	References
Taiwan	Ex situ benthic chambers	Bare sediment <i>H. uninervis</i> , <i>H. ovalis</i>	$0.74 \pm 0.09$ $25.99 \pm 0.96$	$0.62 \pm 0.09$ $4.32 \pm 0.26$	$20.10 \pm 2.84$ $208.21 \pm 6.33$	This study
Taiwan	Open water mass balance	<i>Thalassia</i> , <i>Cymodocea</i>	$42.25 \pm 14.42$	$20.71 \pm 7.13$	$8 \pm 61$	Chou et al., 2023
Mexico	In situ benthic chambers	Bare sediment 2-year <i>H. wrightii</i> 4-year <i>H. wrightii</i> 4-year <i>H. wrightii</i>	$2.13 \pm 0.58$ $13.76 \pm 3.35$ $9.24 \pm 2.34$ $9.34 \pm 0.35$	$0.73 \pm 0.16$ $2.61 \pm 0.40$ $1.60 \pm 0.19$ $2.15 \pm 0.25$	$8.1 \pm 10.9$ $102.4 \pm 31.5$ $72.5 \pm 27.9$ $60.7 \pm 4.7$	Egea et al., 2023
Sweden	Aquatic eddy covariance and benthic chambers	3-year-old restored seagrass ( <i>Z. marina</i> ) 7-year-old restored seagrass ( <i>Z. marina</i> )			$-5 \text{ to } -15$ $-21$	Kindeberg et al., 2024

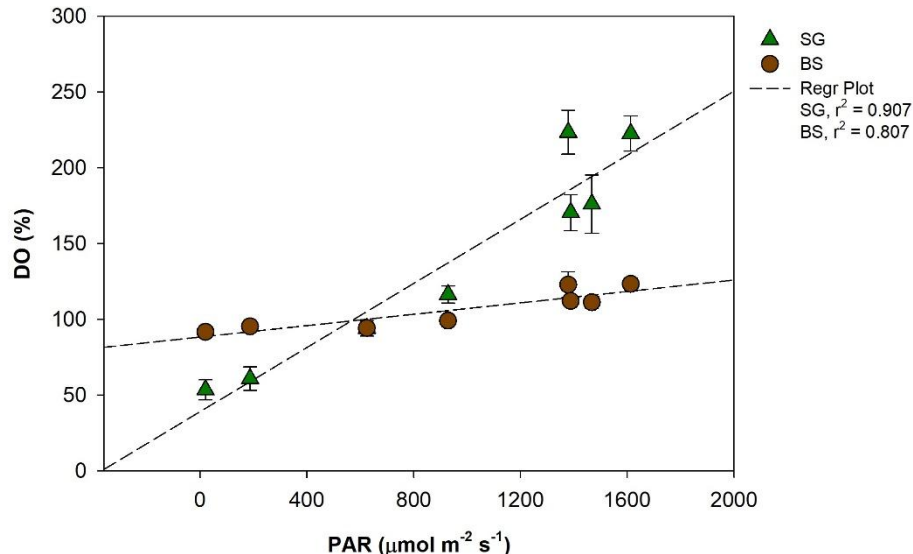
Finland	Aquatic eddy covariance	Bare sediment	1.60	0.82	-0.14	Attard et al., 2019
		<i>Z. marina</i>	3.74	1.71	4.17	
Australia	Ex situ benthic	Bare sediment	2.28	1.26	-2.74	Chen et al., 2019
		<i>Zostera</i> sp.	6.94	2.74	7.12	
		<i>Halophila</i> sp.	2.05	1.60	-13.70	
Tropical Australia	Combined methods	<i>H. uninervis</i>	23.42 ± 3.67	9.63 ± 4.04	50 ± 53	Duarte et al., 2010
Tropical	Combined methods	All species	21 ± 0.6	9 ± 0.6	24 ± 8	Duarte et al., 2010
Global	Combined methods	All species	19 ± 0.5	8 ± 0.4	27 ± 6	Duarte et al., 2010
Spain	In situ benthic chambers	Bare sediment	0.43	0.22	0.27	Barron et al., 2006
		<i>P. oceanica</i>	7.72	3.18	16.44	

313 The daily values of *R* and *GPP* reported in the literature were divided by 24 and 12, respectively, to calculate the  
314 hourly values.

315

316 Key drivers of elevated metabolic rates in tropical meadows include greater PAR availability,  
317 aboveground biomass, and higher temperatures (Ganguly et al., 2017; Ward et al., 2022). Many tropical  
318 species grow near their optimal photosynthetic and physiological conditions (Lee et al., 2007; Koch et al.,  
319 2012), efficiently capturing light in shallow, clear waters, which contributes to higher NEP (Ralph et al.,  
320 2007). In our study, DO variation corresponds to light intensity (Figs. 3 and 7), suggesting that the  
321 elevated GPP observed in seagrass meadows could be driven by higher light intensity. This is likely due  
322 to the relatively lower canopy cover of *H. uninervis* and density in SG, which reduces shading within the  
323 seagrass. As a result, more light penetrates to the leaves, increasing their photosynthetic surface area and  
324 contributing to NEM (Ralph et al., 2007). In contrast, lower respiration rates in the SG area were likely  
325 due to the sediment characteristics and organic matter quality in this habitat. The seagrass beds are situated  
326 in carbonate-rich sediments, which typically contain less organic matter than siliciclastic or muddy  
327 sediments (Belshe et al., 2018; Kindeberg et al., 2018). This limits the availability of substrates for  
328 microbial decomposition. Moreover, the organic matter derived from seagrass detritus is generally more  
329 refractory and less labile, further reducing its accessibility for microbial breakdown and thereby  
330 suppressing heterotrophic respiration (Ren et al., 2024). Although seagrasses are capable of transporting

331 oxygen to their belowground tissues via internal aerenchyma (Borum et al., 2006), which can support  
 332 aerobic respiration, the combined effect of low organic content and poor substrate lability limits microbial  
 333 activity and oxygen consumption.  
 334



335 **Figure 7: Regression plot between photosynthetically active radiation (PAR,  $\mu\text{mol m}^{-2} \text{s}^{-1}$ ) vs**  
 336 **dissolved oxygen (DO, %) in restored seagrass (SG, green triangle) and bare sediment (BS, brown**  
 337 **circle). Error bars represent standard deviation (SD).**  
 338

339  
 340 Several studies indicate that restored seagrass can achieve primary productivity and carbon sequestration  
 341 levels comparable to natural meadows, although recovery depends on the extent of degradation,  
 342 restoration success, and site-specific habitat conditions (Oreska et al., 2017; Marbà et al., 2015). For  
 343 example, long-term research in Florida Bay demonstrated that sediment carbon sequestration rates and  
 344 plant biomass took nearly a decade to match those of natural meadows (Greiner et al., 2013). The ability  
 345 of restored meadows to maintain net autotrophy is crucial for their role as carbon sinks (Kennedy et al.,  
 346 2010). This is particularly relevant for climate change mitigation strategies, where the conservation and  
 347 rehabilitation of this ecosystem are recognized as natural climate solutions (Griscom et al., 2017).  
 348 Nonetheless, a recent investigation on restored seagrass exhibits net heterotrophy, as observed by  
 349 Kindeberg et al. (2024) in both 3-year and 7-year-old meadows in Sweden. A similar pattern also reported

350 in some natural seagrass meadows in Australia (Chen et al., 2019) (Table 1). This discrepancy underscores  
351 the variability in seagrass productivity and metabolic processes based on geographical location and  
352 environmental conditions, highlighting the need for region-specific assessments to fully understand  
353 seagrass ecosystem dynamics. Long-term studies should also consider temporal and annual variations.

#### 354 **4.2 Calcification dynamics in restored seagrass**

355 Our results show that restored seagrass meadows exhibit significantly higher  $\text{CaCO}_3$  cycling — both  
356 formation and dissolution — compared to bare sediments. This corroborates with prior studies, which  
357 documented enhanced carbonate dynamics in vegetated habitats relative to unvegetated sediments. For  
358 instance, *P. oceanica* and *Thalassia testudinum* meadows have been shown to promote both  $\text{CaCO}_3$   
359 production and dissolution (Burdige and Zimmerman, 2002; Barrón et al., 2006), with tropical seagrass  
360 ecosystems displaying similar patterns (Chou et al., 2021; Fan et al., 2024). Further, our data revealed a  
361 typical diurnal pattern, with positive values during daytime (net calcifying) and negative values during  
362 nighttime (net dissolving). These findings align with previous estimates, such as those in Florida Bay,  
363 which reported similar diurnal calcification dynamics (Yates and Halley, 2006).

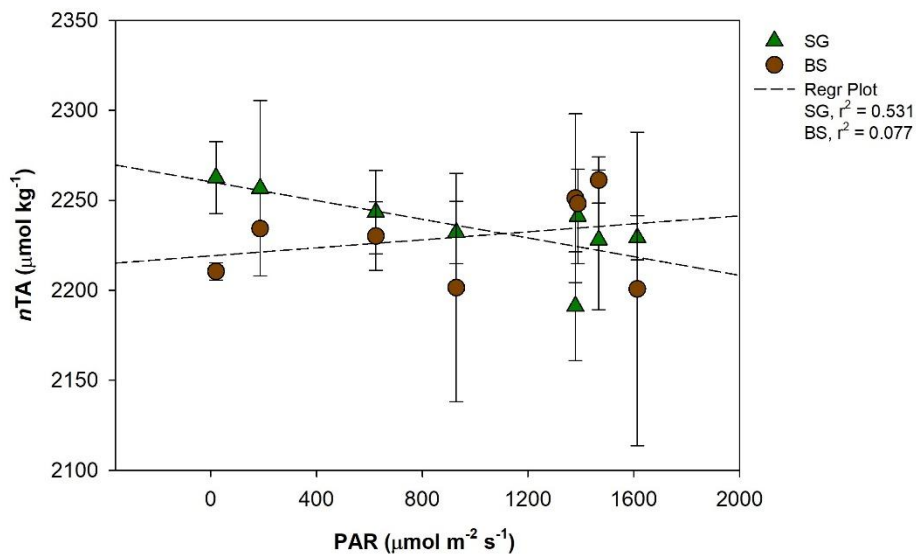
364

365 The variations of  $\text{CaCO}_3$  production and dissolution in surface waters and sediment are related to the  
366 carbon cycle through photosynthesis and respiration (Yates and Halley 2006). During daylight hours,  
367 photosynthesis raises pH and reduces  $\text{CO}_2$  levels in the water, creating favorable conditions for calcium  
368 carbonate precipitation—a process referred to as light-enhanced calcification (Schneider et al., 2009).  
369 We found a significant positive correlation between PAR and  $n\text{TA}$  changes ( $r^2 = 0.52$ ,  $p < 0.05$ ), suggesting  
370 that increased light availability may enhance calcification by photoautotrophs in restored seagrass areas  
371 during the day (Fig. 8). Additionally, our data showed a significant negative correlation between  $n\text{TA}$   
372 flux and NEM ( $r^2 = 0.54$ ,  $p < 0.01$ ), indicating that higher photosynthetic activity (positive NEM) promotes  
373 calcification by consuming TA, while lower NEM or net heterotrophy contributes to TA production,  
374 likely through carbonate dissolution or anaerobic decomposition (Fig. 9). Similar relationships between  
375 photosynthesis and calcification have been reported in marine calcifiers (Mallon et al., 2022), and the  
376 influence of epiphytic organisms in promoting calcification during active photosynthesis has been



377 highlighted in seagrass meadows such as *P. oceanica* (Barrón et al., 2006). At night, carbonate dissolution  
 378 predominates as aerobic respiration produces CO<sub>2</sub> and carbonic acid in sediment porewater (Eyre et al.,  
 379 2014), lowering carbonate saturation and driving mineral dissolution (Burdige and Zimmerman, 2002;  
 380 Burdige et al., 2008; Chou et al., 2021; Fan et al., 2024). The degree of dissolution is directly link to the  
 381 rate of organic matter decomposition, which depends on the quantity of organic matter, its reactivity, and  
 382 oxygen availability (Anderson et al., 2005; Morse et al., 2006). High shoot density and root biomass in  
 383 restored seagrass meadows enhance organic matter supply and decomposition in sediment, further driving  
 384 nighttime dissolution (Holmer et al., 2013).

385



386  
 387 **Figure 8: Regression plot between photosynthetically active radiation (PAR,  $\mu\text{mol m}^{-2} \text{s}^{-1}$ ) vs**  
 388 **normalized total alkalinity (nTA,  $\mu\text{mol kg}^{-1}$ ) in restored seagrass (SG, green triangle) and bare**  
 389 **sediment (BS, brown circle). Error bars represent standard deviation (SD).**

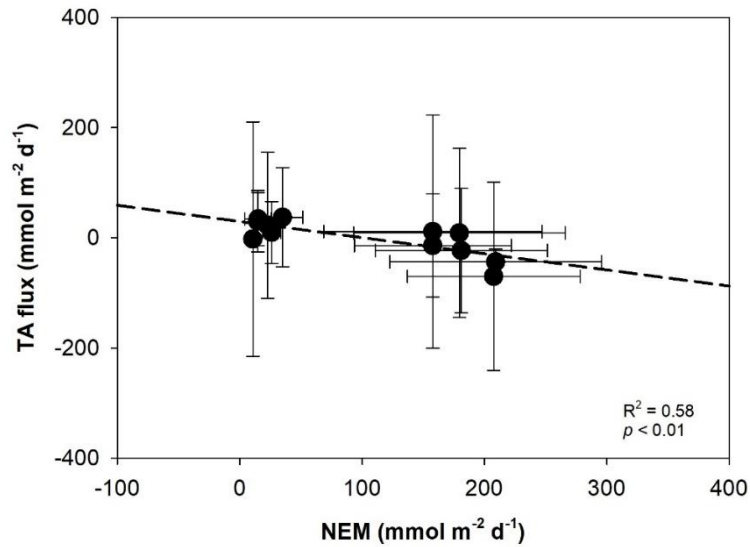


**Figure 9: Linear regression showing the relationship between total alkalinity (TA, mmol m<sup>-2</sup> d<sup>-1</sup>) flux and net ecosystem metabolism (NEM, mmol m<sup>-2</sup> d<sup>-1</sup>) in restored seagrass meadows and bare sediment. Error bars represent standard deviation (SD).**

Over cumulative days, our NEC measurements indicate that restored seagrass meadows support overall net calcification, whereas BS supports net dissolution. Our estimates are similar to those from Australia (Walker et al., 1988) and seven times higher than Mediterranean seagrass net calcification rates (Barrón et al., 2006), which are 295 g CaCO<sub>3</sub> m<sup>-2</sup> yr<sup>-1</sup> (8.8 mmol CaCO<sub>3</sub> m<sup>-2</sup> d<sup>-1</sup>) and 51 g CaCO<sub>3</sub> m<sup>-2</sup> yr<sup>-1</sup> (1.40 mmol CaCO<sub>3</sub> m<sup>-2</sup> d<sup>-1</sup>), respectively. In contrast, our findings are lower than those reported in the Caribbean region of Mexico, where ex situ estimates ranged from 14 to 153 mmol CaCO<sub>3</sub> m<sup>-2</sup> d<sup>-1</sup> (Enriquez and Schubert, 2014). This highlights the enhanced carbonate production potential in tropical seagrass meadows. A positive net calcification system occurs when CaCO<sub>3</sub> precipitation exceeds dissolution within the system (Kleypas et al., 2001; Eyre et al., 2014). Restoration of seagrass meadows provides a substrate for diverse calcifying organisms, including crustose coralline algae, bryozoans, foraminifera, and serpulids, which enhance carbonate production (Beavington-Penney et al., 2005). Epiphytes on seagrass leaves significantly contribute to CaCO<sub>3</sub> production, with tropical seagrass meadows typically supporting higher carbonate loads than temperate ones. Reported production rates

span from 180 g CaCO<sub>3</sub> m<sup>-2</sup> yr<sup>-1</sup> in Jamaica (Land, 1970) to 2800 g CaCO<sub>3</sub> m<sup>-2</sup> yr<sup>-1</sup> in Barbados (Patriquin, 1972), underscoring regional variability in seagrass-associated calcification. Moreover, fluctuations in CO<sub>3</sub><sup>2-</sup> concentrations are crucial in regulating the capacity of calcifying organisms to form CaCO<sub>3</sub>. Our data reveal a higher mean  $\Omega_{Ar}$  in SG ( $3.14 \pm 1$ ) compared to BS ( $2.72 \pm 0.4$ ). Seagrass photosynthesis raises pH and  $\Omega_{Ar}$ , enhancing the calcification of surrounding calcifying organisms (De Beer and Lakrum, 2001). However, the consumption of TA by calcifiers during the calcification process releases CO<sub>2</sub>, potentially counteracting pH increases and partially offsetting the net carbon uptake potential of seagrass ecosystems (Alongi et al., 2008; Mazarrasa et al., 2015; Saderne et al., 2019). This highlights the dual role of seagrass restoration in supporting biodiversity and CO<sub>2</sub> uptake while influencing carbonate and carbon flux dynamics. Although the restored seagrass meadow in our study functions as a net calcifying system, TA fluxes between SG and BS showed no significant difference.

#### 4.3 Net carbon uptake of seagrass restoration

In order to estimate the net carbon uptake potential of seagrass restoration, we applied the photosynthesis-quotient (PQ) of 1 to calculate CO<sub>2</sub> uptake from organic carbon metabolism (Gattuso et al., 1998; Ward et al., 2022). In terms of carbonate dynamics, we applied  $\Phi$ , as described by Humphreys et al. (2018), to calculate the size of CO<sub>2</sub> source or sink for each system. In the SG system, which is net calcifying,  $\Phi$  indicates a CO<sub>2</sub> source, with 0.61 moles of CO<sub>2</sub> released into the seawater for each mole of CaCO<sub>3</sub> precipitated. In contrast, the BS system, which is net dissolving,  $\Phi$  represents a CO<sub>2</sub> sink, with 0.65 moles of CO<sub>2</sub> absorbed for each mole of CaCO<sub>3</sub> dissolved. These values are comparable to previous findings, which reported a CO<sub>2</sub> flux-to-CaCO<sub>3</sub> precipitation ratio of 0.63 (Frankignoulle et al., 1994; Smith, 2013; Mazarrasa et al., 2015). The calculated results show that total carbon uptake from NEM was 208 mmol CO<sub>2</sub> m<sup>2</sup> d<sup>-1</sup> in SG and 20 mmol CO<sub>2</sub> m<sup>2</sup> d<sup>-1</sup> BS. For NEC, the carbon release in SG was 6.6 CO<sub>2</sub> m<sup>2</sup> d<sup>-1</sup>, while for BS, an additional CO<sub>2</sub> uptake was -1.5 mmol CO<sub>2</sub> m<sup>2</sup> d<sup>-1</sup>. Consequently, the net carbon uptake is 202 and 22 mmol CO<sub>2</sub> m<sup>2</sup> d<sup>-1</sup> for SG and BS, respectively. Our results demonstrate that the primary productivity of restored seagrass through photosynthesis exceeds the rates of calcification by 31-fold, suggesting that restored seagrass can act as a net carbon sink. However, further assessments are necessary

435 to capture temporal variations, as our current measurements are based on daily observations and one  
436 season only.

437

#### 438 **4.4 Limitations of ex situ benthic incubation and future research**

439 We tested the ex situ benthic core incubation approach for restored seagrass meadows, drawing from the  
440 existing utilities in some coastal areas and freshwater ecosystems for sulfate and nutrient fluxes (Eyre, et  
441 al., 2005, Chen et al., 2019). Overall, the ex situ benthic incubation method provides a significant  
442 advantage by measuring both organic and inorganic carbon dynamics simultaneously, addressing a  
443 critical gap in previous methods that often overlook carbonate dynamics (Johanssen, 2023). This approach  
444 is also useful for assessing seagrass metabolism in subtidal meadows, where collecting data is challenging  
445 due to high labor costs and weather conditions. Moreover, some in situ autonomous methods are often  
446 expensive and constrained operational periods of only a few weeks due to challenges like sensor error  
447 and biofouling (Yates and Halley, 2003; Takeshita et al., 2016). While this approach provides several  
448 advantages, one notable limitation is its applicability. Currently, the design is primarily suited for small  
449 seagrass, like *H. ovalis*, *H. uninervis*, and *Z. japonica*. It may not be adequate for larger species, like  
450 *Enhalus acoroides* and large *Thalassia hemprichii*, due to differences in size and growth characteristics.  
451 Moreover, we suggest validating the ex situ results with in situ data to ensure comparability with natural  
452 conditions, particularly the effects of light attenuation. Our measurements were obtained under ex-situ  
453 conditions in a shallow water column, which likely exposed the cores to higher irradiance than would be  
454 encountered in situ at different seagrass depths (2–4 m). While previous research has shown that ex situ  
455 and in situ incubations can yield comparable metabolic estimates, supporting the validity of our approach  
456 (Maher and Eyre, 2011), we acknowledge the need for future in situ incubations to more accurately  
457 capture the natural light environment experienced by seagrass leaves. Future research should integrate ex  
458 situ results with in situ data with different geographic and environmental settings to enhance the  
459 generalizability of the findings. This will provide a more accurate assessment of seagrass ecosystems' role  
460 in global carbon cycling and inform more effective coastal management and conservation practices.

## 461 **5 Conclusion**

462 This study investigates the organic carbon metabolism and carbonate dynamics of replanted SG compared  
463 to BS using the ex situ core incubation method. The results show that SG has higher GPP and NEM, while  
464 exhibiting similar NEC, making it a stronger carbon sink than BS. The findings highlight the role of  
465 seagrass restoration in enhancing carbon removal and contribute to a growing body of literature that  
466 highlights the ecological value of restored seagrass meadows. This study represents the first simultaneous  
467 quantitative estimate of the effect of both organic carbon metabolism and carbonate dynamics on carbon  
468 sequestration of restored seagrass in Southeast Asia, providing valuable insights into the region's carbon  
469 dynamics. We emphasize the need for long-term research on metabolic rates and carbonate dynamics to  
470 account for temporal variations and to fully understand the implications of these processes in carbon  
471 sequestration. This will also help optimize restoration strategies aimed at maximizing carbon sink  
472 potential and mitigating ocean acidification. Furthermore, ex situ benthic incubation proves to be a  
473 valuable tool for assessing carbon fluxes in seagrass meadows, particularly those dominated by pioneering  
474 species, although further in situ assessments are necessary for comprehensive validation.

## 475 **Author contribution**

476 Wen-Chen Chou (WCC) and Jian-Jhih Chen (JJC) conceptualized the research and spearheaded the  
477 implementation. JJC, Mariche B. Natividad (MBN), and Hsin-Yu Chou facilitated sample collection and  
478 analysis. MBN and JJC performed the data analysis, drafted the manuscript, and its revision. WCC and  
479 Lan-Feng Fan reviewed and revised the manuscript. All authors were involved in the finalization of the  
480 manuscript.

## 481 **Competing interest**

482 The authors declare that they have no conflict of interest.

## 483 **Data availability**

484 The data supporting the findings of this study are available in the DRYAD repository at  
485 <https://doi.org/10.5061/dryad.d7wm37qd0> (Natividad et al., 2025).

486 **Acknowledgment**

487 We are grateful to Hsin-Chiao Chang, Yuhann Yokie-Tai, Ping-Chun Chen, and Xin-Yi Wang for the  
488 field sampling and laboratory assistance, and to Adrian Lansigan for generating the map.

489 **Financial support**

490 This work was funded by the National Science and Technology Council of Taiwan under grant numbers  
491 NSTC 113-2119-M-019-008 and NSTC 113-2611-M-019-011, given to WCC.

## 492 References

- 493 Allen Coral Atlas: Imagery, maps and monitoring of the world's tropical coral reefs. Zendodo.  
494 [doi.org/10.5281/zenodo.3833242](https://doi.org/10.5281/zenodo.3833242), 2020.
- 495 Alongi, D.M., Trott, L.A., Undu, M.C., and Tirendi, F.: Benthic microbial metabolism in seagrass  
496 meadows along a carbonate gradient in Sulawesi, Indonesia. *Aquat. Microb. Ecol.*, 51:141–152.  
497 [doi:10.3354/ame01191](https://doi.org/10.3354/ame01191), 2008.
- 498 Apostolaki, E. T., Holmer, M., Marbà, N., and Karakassis, I.: Metabolic Imbalance in Coastal Vegetated  
499 (*Posidonia oceanica*) and Unvegetated Benthic Ecosystems. *Ecosystems*, 13(3), 459–471.  
500 [doi.org/10.1007/s10021-010-9330-9](https://doi.org/10.1007/s10021-010-9330-9), 2010.
- 501 Barrón, C., Duarte, C. M., Frankignoulle, M., and Borges, A. V.: Organic carbon metabolism and  
502 carbonate dynamics in a Mediterranean seagrass (*Posidonia oceanica*), meadow. *Estuar. Coasts.*, 29  
503 (3), 417–426. [doi.org/10.1007/bf02784990](https://doi.org/10.1007/bf02784990), 2006.
- 504 Beavington-penney, S. J., Wright, V. P., & Racey, A.: Sediment production and dispersal on foraminifera-  
505 dominated early Tertiary ramps: The Eocene El Garia Formation, Tunisia. *Sedimentology*, 52(3),  
506 537–569. [doi.org/10.1111/j.1365-3091.2005.00709.x](https://doi.org/10.1111/j.1365-3091.2005.00709.x), 2005.
- 507 Belshe, E. F., Hoeijmakers, D., Herran, N., Mtolera, M., & Teichberg, M.: Seagrass community-level  
508 controls over organic carbon storage are constrained by geophysical attributes within meadows of  
509 Zanzibar, Tanzania. *Biogeosciences*, 15(14), 4609–4626. <https://doi.org/10.5194/bg-15-4609-2018>,  
510 2018.
- 511 Berg, P., Huettel, M., Glud, R. N., Reimers, C. E., and Attard, K. M. Aquatic Eddy Covariance: The  
512 method and its contributions to defining oxygen and carbon fluxes in marine environments. *Ann. Rev.*  
513 *Mar. Sci.*, 14(1), 431–455. [doi.org/10.1146/annurev-marine-042121-012329](https://doi.org/10.1146/annurev-marine-042121-012329), 2022.
- 514 Burdige, D. J. and Zimmerman, R.C.: Impact of sea grass density on carbonate dissolution in Bahamian  
515 sediments. *Limnol. Oceanogr.*, 47(6), 1751–1763. doi: 10.4319/lo.2002.47.6.1751, 2002.
- 516 Burdige, D. J., Zimmerman, R. C., and Hu, X.: Rates of carbonate dissolution in permeable sediments  
517 estimated from porewater profiles: the role of sea grasses. *Limnol. Oceanogr.*, 53: 549–565.  
518 [doi:10.2307/40006440](https://doi.org/10.2307/40006440), 2008.



519 Campbell, S., Miller, C., Steven, A., and Stephens, A.: Photosynthetic responses of two temperate  
 520 seagrasses across a water quality gradient using chlorophyll fluorescence. *J. Exp. Mar. Biol. Ecol.*,  
 521 291(1), 57–78. [doi.org/10.1016/s0022-0981\(03\)00090-x](https://doi.org/10.1016/s0022-0981(03)00090-x), 2003.

522 Chen, J., Wells, N., Erler, D., and Eyre, B.: Importance of habitat diversity to changes in benthic  
 523 metabolism over land-use gradients: evidence from three subtropical estuaries. *Mar. Ecol. Prog. Ser.*,  
 524 631, 31–47. [doi.org/10.3354/meps13147](https://doi.org/10.3354/meps13147), 2019.

525 Chou, W., Fan, L., Hung, C., Shih, Y., Huang, W., Lui, H., and Chen, T.: Dynamics of O<sub>2</sub> and pCO<sub>2</sub> in a  
 526 Southeast Asia seagrass meadow: Metabolic rates and carbon sink capacity. *Front. Mar. Sci.*, 10.  
 527 [doi.org/10.3389/fmars.2023.1076991](https://doi.org/10.3389/fmars.2023.1076991), 2023.

528 Chou, W., Fan, L., Yang, C., Chen, Y., Hung, C., Huang, W., Shih, Y., Soong, K., Tseng, H., Gong, G.,  
 529 Chen, H., and Su, C.: A unique DIEL pattern in carbonate chemistry in the seagrass meadows of  
 530 Dongsha Island: the enhancement of metabolic carbonate dissolution in a semienclosed lagoon. *Front.*  
 531 *Mar. Sci.*, 8. [doi.org/10.3389/fmars.2021.717685](https://doi.org/10.3389/fmars.2021.717685), 2021.

532 Chou, W.-C., Chu, H.-C., Chen, Y.-H., Syu, R.-W., Hung, C.-C., and Soong, K.: Short-term variability of  
 533 carbon chemistry in two contrasting seagrass meadows at Dongsha island: implications for pH  
 534 buffering and CO<sub>2</sub> sequestration. *Estuar. Coast. Shelf Sci.*, 210, 36–44. doi:  
 535 10.1016/j.ecss.2018.06.006, 2018.

536 Clayton, T. D. and Byrne, R. H.: Spectrophotometric seawater pH measurements: total hydrogen ion  
 537 concentration scale calibration of m-cresol purple and at-sea results. *Deep-Sea Res. I: Oceanogr. Res.*  
 538 *Pap.*, 40(10), 2115–2129. [doi.org/10.1016/0967-0637\(93\)90048-8](https://doi.org/10.1016/0967-0637(93)90048-8), 1993.

539 De Beer, D., and A. W. D. Larkum.: Photosynthesis and calcification in the calcifying algae *Halimeda*  
 540 *discoidea* studied with microsensors. *Plant Cell Environ.* 24: 1209– 1217. doi:10.1046/j.1365-  
 541 3040.2001.00772.x, 2001.

542 Dickson, A.G. and Millero, F.J.: A Comparison of the Equilibrium Constants for the Dissociation of  
 543 Carbonic Acid in Seawater Media. *Deep-Sea Res. I: Oceanogr. Res. Pap.*, 34, 1733-1743.  
 544 [doi.org/10.1016/0198-0149\(87\)90021-5](https://doi.org/10.1016/0198-0149(87)90021-5), 1987.

545 Dickson, A.G., Sabine, C.L. and Christian, J.R. (Eds.): Guide to best practices for ocean CO<sub>2</sub>  
 546 measurements. PICES Special Publication 3, 191 pp., 2007.

547 Duarte, C. M. and Krause-Jensen, D.: Export from Seagrass Meadows Contributes to Marine Carbon  
 548 Sequestration, *Frontiers in Marine Science*, 4, 13, doi.org/10.3389/fmars.2017.00013, 2017.

549 Duarte, C. M., Sintes, T., and Marbà, N.: Assessing the CO<sub>2</sub> capture potential of seagrass restoration  
 550 projects. *J. Appl. Ecol.*, 50(6), 1341–1349. doi.org/10.1111/1365-2664.12155, 2013.

551 Duarte, C. M., Marbà, N., Gacia, E., Fourqurean, J. W., Beggins, J., Barrón, C., and Apostolaki, E. T.:  
 552 Seagrass community metabolism: Assessing the carbon sink capacity of seagrass meadows. *Global*  
 553 *Biogeochem. Cy.*, 24(4). doi.org/10.1029/2010gb003793, 2010.

554 Duarte, C. M., Middelburg, J. J., and Caraco, N.: Major role of marine vegetation on the oceanic carbon  
 555 cycle. *Biogeosciences*, 2(1), 1–8. doi.org/10.5194/bg-2-1-2005, 2005.

556 Egea, L., Infantes, E., & Jiménez-Ramos, R. (2023). Loss of POC and DOC on seagrass sediments by  
 557 hydrodynamics. *Sci. Total Environ.*, 901, 165976. doi.org/10.1016/j.scitotenv.2023.165976

558 Enríquez, S. and Schubert, N.: Direct contribution of the seagrass *Thalassia testudinum* to lime mud  
 559 production. *Nat. Commun.* **5**, 3835. doi.org/10.1038/ncomms4835, 2014.

560 Eyre, B.D., Rysgaard, S., Dalsgaard, T., Christensen, P.B.: Comparison of isotope pairing and N<sub>2</sub>: Ar  
 561 methods for measuring sediment denitrification—assumptions, modifications, and implications.  
 562 *Estuaries* 25: 1077–1087, doi.org/10.4319/lo.2002.47.4.1043, 2002

563 Eyre, B. D. and Ferguson, A. J. P.: Benthic metabolism and nitrogen cycling in a subtropical east  
 564 Australian estuary (Brunswick): Temporal variability and controlling factors. *Limnol. Oceanogr.*,  
 565 50(1), 81–96. doi.org/10.4319/lo.2005.50.1.0081, 2005.

566 Eyre, B. D., A. J. P. Ferguson, A. Webb, D. Maher, and J. M. Oakes.: Denitrification, N-fixation and  
 567 nitrogen and phosphorus fluxes in different benthic habitats and their contribution to the nitrogen and  
 568 phosphorus budgets of a shallow oligotrophic sub-tropical coastal system (southern Moreton Bay,  
 569 Australia). *Biogeochemistry* 102: 111–133. doi:10.1007/s10533-010-9425-6, 2011.

570 Eyre, B. D., Andersson, A. J., & Cyronak, T.: Benthic coral reef calcium carbonate dissolution in an  
 571 acidifying ocean. *Nat. Clim. Change*, 4(11), 969–976. doi.org/10.1038/nclimate2380, 2014.

572 Fan, L.-F., Kang, E.-C., Natividad, M. B., Hung, C.-C., Shih, Y.-Y., Huang, W.-J., & Chou, W.-C.: The  
 573 role of benthic TA and DIC fluxes on carbon sequestration in seagrass meadows of Dongsha Island.  
 574 *J. Mar. Sci. Eng.*, 12, 2061. doi.org/10.3390/jmse12112061, 2024.

575 Ferguson, A., Eyre, B., and Gay, J.: Benthic nutrient fluxes in euphotic sediments along shallow sub-  
576 tropical estuaries, northern New South Wales, Australia. *Aquat. Microb. Ecol.*, 37, 219–235.  
577 [doi.org/10.3354/ame037219](https://doi.org/10.3354/ame037219), 2004.

578 Frankignoulle, M., Canon, C., and Gattuso, J.-P.: Marine calcification as a source of carbon dioxide:  
579 Positive feedback of increasing atmospheric CO<sub>2</sub>, *Limnol. Oceanogr.*, 39(2), 458–462, 1994.

580 Fourqurean, J. W., Duarte, C. M., Kennedy, H., Marbà, N., Holmer, M., Mateo, M. A., Apostolaki, E. T.,  
581 Kendrick, G. A., Krause-Jensen, D., McGlathery, K. J., & Serrano, O.: Seagrass ecosystems as a  
582 globally significant carbon stock. *Nat. Geosci.*, 5(7), 505–509. [doi.org/10.1038/ngeo1477](https://doi.org/10.1038/ngeo1477), 2012.

583 Ganguly, D., Singh, G., Ramachandran, P., Selvam, A.P., Banerjee, K., and Ramachandran, R.: Seagrass  
584 metabolism and carbon dynamics in a tropical coastal embayment. *Ambio*. Oct;46(6):667-679. doi:  
585 10.1007/s13280-017-0916-8. Epub 2017 Mar 31. PMID: 28364264; PMCID: PMC5595744., 2017

586 Gazeau, F., Duarte, C. M., Gattuso, J., Barrón, C., Navarro, N., Ruiz, S., Prairie, Y. T., Calleja, M., Delille,  
587 B., Frankignoulle, M., and Borges, A. V.: Whole-system metabolism and CO<sub>2</sub> fluxes in a  
588 Mediterranean Bay dominated by seagrass beds (Palma Bay, NW Mediterranean). *Biogeosciences*,  
589 2(1), 43–60. [doi.org/10.5194/bg-2-43-2005](https://doi.org/10.5194/bg-2-43-2005), 2005

590 Greiner, J. T., McGlathery, K. J., Gunnell, J., and McKee, B. A.: Seagrass restoration enhances “Blue  
591 carbon” sequestration in coastal waters. *PLoS ONE*, 8(8), e72469.  
592 [doi.org/10.1371/journal.pone.0072469](https://doi.org/10.1371/journal.pone.0072469), 2013.

593 Griscom, B. W., Adams, J., Ellis, P. W., Houghton, R. A., Lomax, G., Miteva, D. A., Schlesinger, W. H.,  
594 Shoch, D., Siikamäki, J. V., Smith, P., Woodbury, P., Zganjar, C., Blackman, A., Campari, J., Conant,  
595 R. T., Delgado, C., Elias, P., Gopalakrishna, T., Hamsik, M. R., . . . Fargione, J.: Natural climate  
596 solutions. *P. Natl. A Sci*, 114(44), 11645–11650. [doi.org/10.1073/pnas.1710465114](https://doi.org/10.1073/pnas.1710465114), 2017.

597 Hendriks, I. E., Olsen, Y. S., Ramajo, L., Basso, L., Steckbauer, A., Moore, T. S., Howard, J. and Duarte,  
598 C. M.: Photosynthetic activity buffers ocean acidification in seagrass meadows, *Biogeosciences*,  
599 11(2), 333, 2014.

600 Howard, J. L., Creed, J. C., Aguiar, M. V. P., and Fourqurean, J. W.: CO<sub>2</sub> released by carbonate sediment  
601 production in some coastal areas may offset the benefits of seagrass “Blue Carbon” storage. *Limnol.*  
602 *Oceanogr.*, 63(1), 160–172. [doi.org/10.1002/lno.10621](https://doi.org/10.1002/lno.10621), 2017.

603 Humphreys, M.P., Daniels, C. J., Wolf-Gladrow, D. A., Tyrrell, T., & Achterberg, E. P.: On the influence  
 604 of marine biogeochemical processes over CO<sub>2</sub> exchange between the atmosphere and ocean. *Marine*  
 605 *Chemistry*, 199, 1–11. <https://doi.org/10.1016/j.marchem.2017.12.006>, 2018.

606 Johannessen, S. C.: How to quantify blue carbon sequestration rates in seagrass meadow sediment:  
 607 geochemical method and troubleshooting. *Carbon Footprints*, 2(4). [doi.org/10.20517/cf.2023.37](https://doi.org/10.20517/cf.2023.37),  
 608 2023.

609 Juska, I. and Berg, P.: Variation in seagrass meadow respiration measured by aquatic eddy covariance.  
 610 *Limnol. Oceanogr. Lett.* 7(5), 410–418. [doi.org/10.1002/lol2.10276](https://doi.org/10.1002/lol2.10276), 2022.

611 Kennedy, H., Beggins, J., Duarte, C. M., Fourqurean, J. W., Holmer, M., Marbà, N., and Middelburg, J.  
 612 J.: Seagrass sediments as a global carbon sink: Isotopic constraints. *Global Biogeochem. Cy.*, 24(4).  
 613 [doi.org/10.1029/2010gb003848](https://doi.org/10.1029/2010gb003848), 2010.

614 Kindeberg, T., Attard, K. M., Hüller, J., Müller, J., Quintana, C. O., and Infantes, E.: Structural complexity  
 615 and benthic metabolism: resolving the links between carbon cycling and biodiversity in restored  
 616 seagrass meadows. *Biogeosciences*, 21(7), 1685–1705. [doi.org/10.5194/bg-21-1685-2024](https://doi.org/10.5194/bg-21-1685-2024), 2024.

617 Kindeberg, T., Bates, N. R., Courtney, T. A., Cyronak, T., Griffin, A., Mackenzie, F. T., et al.: Porewater  
 618 carbonate chemistry dynamics in a temperate and a subtropical seagrass system. *Aquat. Geochem.* 26,  
 619 375–399. doi: 10.1007/s10498-020-09378-8, 2020.

620 Kindeberg, T., Ørberg, S. B., Röhr, M. E., Holmer, M., & Krause-Jensen, D.: Sediment stocks of carbon,  
 621 nitrogen, and phosphorus in Danish eelgrass meadows. *Front. Mar. Sci.*, 5, 474.  
 622 <https://doi.org/10.3389/fmars.2018.00474>, 2018.

623 Kleypas, J. A., Buddemeier, R. W., and Gattuso, J. P.: The future of coral reefs in an age of global  
 624 change. *Int. J. Earth Sci.*, 90, 426–437, [doi.org/10.1007/s005310000125](https://doi.org/10.1007/s005310000125), 2001.

625 Koch, M., Bowes, G., Ross, C., and Zhang, X.: Climate change and ocean acidification effects on  
 626 seagrasses and marine macroalgae. *Glob. Change Biol.*, 19(1), 103–132. [doi.org/10.1111/j.1365-](https://doi.org/10.1111/j.1365-2486.2012.02791.x)  
 627 [2486.2012.02791.x](https://doi.org/10.1111/j.1365-2486.2012.02791.x), 2012.

628 Kraemer, G.P. and Alberte, R.S.: Age-related patterns of metabolism and biomass in subterranean tissues  
 629 of *Zostera marina* L. (eelgrass). *Mar. Ecol. Prog. Ser.*, 95: 193–203, 1993.

630 Land, L. S. Carbonate mud; production by epibiont growth on *Thalassia testudinum*. J. Sediment.  
631 Res., 40, 1361–1363. [doi.org/10.1306/74D721B7-2B21-11D7-8648000102C1865D](https://doi.org/10.1306/74D721B7-2B21-11D7-8648000102C1865D), 1970.

632 Lee, K., Park, S. R., and Kim, Y. K.: Effects of irradiance, temperature, and nutrients on growth dynamics  
633 of seagrasses: A review. J. Exp. Mar. Biol. Ecol., 350(1–2), 144–175.  
634 [doi.org/10.1016/j.jembe.2007.06.016](https://doi.org/10.1016/j.jembe.2007.06.016), 2007.

635 Macreadie, P. I., Serrano, O., Maher, D. T., Duarte, C. M., and Beardall, J.: Addressing calcium carbonate  
636 cycling in blue carbon accounting. Limnol. Oceanogr. Lett., 2(6), 195–201.  
637 [doi.org/10.1002/lol2.10052](https://doi.org/10.1002/lol2.10052), 2017.

638 Maher, D., & Eyre, B.: Benthic carbon metabolism in southeast Australian estuaries: habitat importance,  
639 driving forces, and application of artificial neural network models. Mar. Ecol. Prog. Ser., 439, 97–  
640 115. [doi.org/10.3354/meps09336](https://doi.org/10.3354/meps09336), 2011.

641 Mallon, J., Cyronak, T., Hall, E. R., Banaszak, A. T., Exton, D. A., and Bass, A. M.: Light-driven dynamics  
642 between calcification and production in functionally diverse coral reef calcifiers. Limnol. and  
643 Oceanogr., 67(2), 434–449. [doi.org/10.1002/lno.12002](https://doi.org/10.1002/lno.12002), 2002.

644 Marbà, N., Arias-Ortiz, A., Masqué, P., Kendrick, G. A., Mazarrasa, I., Bastyan, G. R., Garcia-Orellana,  
645 J., and Duarte, C. M.: Impact of seagrass loss and subsequent revegetation on carbon sequestration  
646 and stocks. J. Ecol., 103(2), 296–302. [doi.org/10.1111/1365-2745.12370](https://doi.org/10.1111/1365-2745.12370), 2015.

647 Mazarrasa, I., Marbà, N., Lovelock, C. E., Serrano, O., Lavery, P. S., Fourqurean, J. W., Kennedy, H.,  
648 Mateo, M. Á., Krause-Jensen, D., Steven, A. D. L., and Duarte, C. M.: Seagrass meadows as a globally  
649 significant carbonate reservoir. Biogeosciences, 12(16), 4993–5003. [doi.org/10.5194/bg-12-4993-](https://doi.org/10.5194/bg-12-4993-2015)  
650 [2015](https://doi.org/10.5194/bg-12-4993-2015), 2015.

651 Mcleod, E., Chmura, G. L., Bouillon, S., Salm, R., Björk, M., Duarte, C. M., Lovelock, C. E., Schlesinger,  
652 W. H., and Silliman, B. R.: A blueprint for blue carbon: toward an improved understanding of the role  
653 of vegetated coastal habitats in sequestering CO<sub>2</sub>. Front. Ecol. Environ., 9(10), 552–560.  
654 [doi.org/10.1890/110004](https://doi.org/10.1890/110004), 2011.

655 Mehrbach, C., Culberson, C. H., Hawley, J. E., and Pytkowicz, R. M.: Measurement of the apparent  
656 dissociation constants of carbonic acid in seawater at atmospheric pressure<sup>1</sup>. Limnol. Oceanogr.,  
657 18(6), 897–907. [doi.org/10.4319/lo.1973.18.6.0897](https://doi.org/10.4319/lo.1973.18.6.0897), 1973.

658 Odum, H. T.: Primary production in flowing waters, *Limnol. Oceanogr.*, 1(2), 102–117, 1956.

659 Olivé, I., Silva, J., Costa, M. M., and Santos, R.: Estimating seagrass community metabolism using benthic  
660 chambers: The effect of incubation time. *Estuar. Coasts*, 39(1), 138–144. [doi.org/10.1007/s12237-](https://doi.org/10.1007/s12237-015-9973-z)  
661 [015-9973-z](https://doi.org/10.1007/s12237-015-9973-z), 2016.

662 Oreska, M. P. J., Wilkinson, G. M., McGlathery, K. J., Bost, M., and McKee, B. A.: Non-seagrass carbon  
663 contributions to seagrass sediment blue carbon. *Limnol. Oceanogr.*, 63(S1).  
664 [doi.org/10.1002/lno.10718](https://doi.org/10.1002/lno.10718), 2017.

665 Ortégón-Aznar, I., Chuc-Contreras, A., & Collado-Vides, L. Calcareous green algae standing stock in a  
666 tropical sedimentary coast. *J. Appl. Phycol.*, 29, 2685–2693. [doi.org/10.1007/s10811-017-1057-y](https://doi.org/10.1007/s10811-017-1057-y),  
667 2017.

668 Orth, R. J., Carruthers, T. J. B., Dennison, W. C., Duarte, C. M., Fourqurean, J. W., Heck, K. L., Hughes,  
669 A. R., Kendrick, G. A., Kenworthy, W. J., Olyarnik, S., Short, F. T., Waycott, M., and Williams, S.  
670 L.: A global crisis for seagrass ecosystems. OUP Academic. [doi.org/10.1641/0006-3568\(2006\)56](https://doi.org/10.1641/0006-3568(2006)56),  
671 2006.

672 Patriquin, D.G: The origin of nitrogen and phosphorus for growth of the marine angiosperm *Thalassia*  
673 *testudinum*. *Mar. Biol.* 15, 35–46. [doi.org/10.1007/BF00347435](https://doi.org/10.1007/BF00347435), 1972.

674 Pelletier, G., Lewis, E., and Wallace, D.: *CO2SYS. XLS: A Calculator for the CO<sub>2</sub> System in Seawater for*  
675 *Microsoft Excel/VBA. Version 16*. Washington, DC: Washington State Department of Ecology, 2011

676 Perry, C., & Beavington-Penney, S.: Epiphytic calcium carbonate production and facies development  
677 within sub-tropical seagrass beds, Inhaca Island, Mozambique. *Sedimentary Geol.*, 174(3–4), 161–  
678 176. [doi.org/10.1016/j.sedgeo.2004.12.003](https://doi.org/10.1016/j.sedgeo.2004.12.003), 2005.

679 Ralph, P., Durako, M., Enríquez, S., Collier, C., and Doblin, M.: Impact of light limitation on seagrasses.  
680 *J. Exp. Mar. Biol. Ecol.*, 350(1–2), 176–193. [doi.org/10.1016/j.jembe.2007.06.017](https://doi.org/10.1016/j.jembe.2007.06.017), 2007.

681 Ren, Y., Liu, S., Luo, H., Jiang, Z., Liang, J., Wu, Y., Huang, X., & Macreadie, P. I.: Seagrass decline  
682 weakens sediment organic carbon stability. *Sci. Total Environ.*, 937, 173523.  
683 <https://doi.org/10.1016/j.scitotenv.2024.173523>, 2024.

684 Rheuban, J. E., Berg, P. and McGlathery, K. J.: Ecosystem metabolism along a colonization gradient of  
685 eelgrass (*Zostera marina*) measured by eddy correlation, *Limnol. Oceanogr.*, 59(4), 1376–1387, 2014.

686 Roth, F., Wild, C., Carvalho, S., Rådecker, N., Voolstra, C. R., Kürten, B., Anlauf, H., El-Khaled, Y. C.,  
687 Carolan, R., and Jones, B. H.: An in situ approach for measuring biogeochemical fluxes in structurally  
688 complex benthic communities. *Methods Ecol. Evol.*, 10(5), 712–725. [doi.org/10.1111/2041-](https://doi.org/10.1111/2041-210x.13151)  
689 [210x.13151](https://doi.org/10.1111/2041-210x.13151), 2019.

690 Saderne, V., Geraldi, N.R., Macreadie, P.I. *et al.*: Role of carbonate burial in Blue Carbon budgets. *Nat*  
691 *Commun.*, 10, 1106, [doi.org/10.1038/s41467-019-08842-6](https://doi.org/10.1038/s41467-019-08842-6), 2019.

692 Schneider, K., Levy, O., Dubinsky, Z., & Erez, J.: In situ diel cycles of photosynthesis and calcification in  
693 hermatypic corals. *Limnol. Oceanogr.*, 54(6), 1995–2002. [doi.org/10.4319/lo.2009.54.6.1995](https://doi.org/10.4319/lo.2009.54.6.1995), 2009.

694 Smith, S. V.: Parsing the oceanic calcium carbonate cycle: a net atmospheric carbon dioxide source, or a  
695 sink? Land O e-Books. Association for the Sciences of Limnology and Oceanography (ASLO) Waco,  
696 TX, doi:10.4319/svsmith.2013.978-0-9845591-2-1, 2013.

697 Takeshita, Y., W. McGillis, E.M. Briggs, A.L. Carter, E.M. Donham, T.R. Martz, N.N. Price, and J.E.  
698 Smith.: Assessment of net community production and calcification of a coral reef using a boundary  
699 layer approach. *J. Geophys. Res-Oceans*. 121: 5655–5671, 2016.

700 Trentman, M. T., Hall Jr., R. O., and Valett, H. M.: Exploring the mismatch between the theory and  
701 application of photosynthetic quotients in aquatic ecosystems. *Limnol. and Oceanogr. Lett.*, 8, 565–  
702 579, [doi.org/10.1002/lol2.10326](https://doi.org/10.1002/lol2.10326), 2023.

703 Van Dam, B. R., Lopes, C., Osburn, C. L., and Fourqurean, J. W.: Net heterotrophy and carbonate  
704 dissolution in two subtropical seagrass meadows. *Biogeosciences*, 16(22), 4411–4428.  
705 [doi.org/10.5194/bg-16-4411-2019](https://doi.org/10.5194/bg-16-4411-2019), 2019.

706 Van Dam, B. R., Zeller, M. A., Lopes, C., Smyth, A. R., Böttcher, M. E., Osburn, C. L., Zimmerman, T.,  
707 Präfroch, D., Fourqurean, J. W., and Thomas, H.: Calcification-driven CO<sub>2</sub> emissions exceed “Blue  
708 Carbon” sequestration in a carbonate seagrass meadow. *Sci. Adv.*, 7(51).  
709 [doi.org/10.1126/sciadv.abj1372](https://doi.org/10.1126/sciadv.abj1372), 2021.

710 Walker, D. & Woelkerling, W. Quantitative study of sediment contribution by epiphytic coralline red algae  
711 in seagrass meadows in Shark Bay, Western Australia. *Mar. Ecol. Prog. Ser.* **43**, 71–77 (1988).

712 Ward, M., Kindinger, T. L., Hirsh, H. K., Hill, T. M., Jellison, B. M., Lummis, S., Rivest, E. B.,  
713 Waldbusser, G. G., Gaylord, B., and Kroeker, K. J.: Reviews and syntheses: Spatial and temporal



714 patterns in seagrass metabolic fluxes, *Biogeosciences*, 19, 689–699, doi.org/10.5194/bg-19-689-2022,  
715 2022.

716 Waycott, M., Duarte, C. M., Carruthers, T. J. B., Orth, R. J., Dennison, W. C., Olyarnik, S., Calladine, A.,  
717 Fourqurean, J. W., Heck, K. L., Hughes, A. R., Kendrick, G. A., Kenworthy, W. J., Short, F. T., and  
718 Williams, S. L.: Accelerating loss of seagrasses across the globe threatens coastal ecosystems. *P. Natl.*  
719 *A. Sci.*, 106(30), 12377–12381. [doi.org/10.1073/pnas.0905620106](https://doi.org/10.1073/pnas.0905620106), 2009.

720 Yang, Y.-P., Fong, S.-C., and Liu H.-Yih.: Taxonomy and distribution of seagrasses in Taiwan. *Taiwania*,  
721 47(1):54-61, 2002.

722 Yates, K.K. and Halley, R.B.: Measuring coral reef community metabolism using new benthic chamber  
723 technology. *Coral Reefs*, 22, 247–255. [doi.org/10.1007/s00338-003-0314-5](https://doi.org/10.1007/s00338-003-0314-5), 2003.

724 Yates, K.K. and Halley, R.B.: Diurnal variation in rates of calcification and carbonates sediment  
725 dissolution in Florida Bay. *Estuar. Coasts*, 29:24–39. 2006.

726 Zeebe, R. E., and Wolf-Gladrow, D.A.: *CO<sub>2</sub> in Seawater: Equilibrium, Kinetics, Isotopes*, Elsevier  
727 *Oceanogr. Ser.*, vol. 65, 346 pp., Elsevier, Amsterdam, 2001.